Dynamics of the last ice sheet on the northern fringe of Poland: reconstruction inferred from landform analysis and ^{10}Be surface exposure dating

Karol Tylmann[1*], Vincent Rinterknecht[2], Piotr P. Woźniak[1], Damian Moskalewicz[1], Aleksandra Bielicka-Giełdoń[3], ASTER Team[2]

[1]*Department of Geomorphology and Quaternary Geology, University of Gdańsk, Poland*
[2]*Aix Marseille Univ., CNRS, IRD, INRAE, CEREGE, France*
[3]*Department of General and Inorganic Chemistry, University of Gdańsk, Poland*

** corresponding Author (k.tylmann@ug.edu.pl)*

ASTER Team: Georges Aumaître, Karim Keddadouche, Fawzi Zaïdi

Non-peer reviewed preprint submitted to EarthArXiv

Submitted to *Quaternary International* June 25th, 2025

Highlights

- Dynamic palaeo-ice margin oscillations on the northern fringe of Poland.
- The main ice margin positions dated between ~17.5 ka and ~15 ka.
- Asynchronous ice streams/ice lobes.
- Meltwater within the ice sheet triggering ice margin oscillations.
- Impeded correlation of particular ice-marginal formations along the southern FIS.

Key words:

Fennoscandian Ice Sheet, LiDAR DEM, erratic boulders, surface exposure dating, MIS 2

Abstract

The paper presents new results of glacial landforms mapping and analysis based on high-resolution Digital Elevation Model (DEM), and ^{10}Be surface exposure dating of erratic boulders on the northern fringe of Poland. We aimed to reconstruct the main ice-marginal positions, local ice flow directions and timing of the ice margin oscillations during the last deglaciation. A total number of 715 glacial landforms has been mapped, including: 274 moraine ridges, 68 subglacial lineations, 74 overridden moraines, 52 eskers, 169 kames, 14 zones of hummocky moraines, 47 subglacial valleys, 5 subglacial meltwater corridors (SMCs), and 12 ice-marginal valleys. Nine erratic boulders have been dated giving ^{10}Be age range between 2.2 ± 0.3 ka and 17.8 ± 1.8 ka with the most reliable ages between 12.5 ± 1.1 ka and 17.8 ± 1.8 ka. Our results suggest dynamic oscillations of the ice sheet with episodes of the ice margin retreat, stillstands and re-advances. The Gardno moraines, described in the literature as a distinct ice-marginal belt correlated with the last Pleistocene ice re-advance in the Polish Lowland, are in fact diversified ice-marginal landsystems representing discontinuous and asynchronous ice sheet dynamics of particular ice streams/ice lobes with the main ice margin positions dated between ~17.5 ka and ~15 ka. The significant occurrence of meltwater-related glacial landforms and deposits in the study area suggests the presence of large volumes of meltwater within the ice sheet leading to the development of intensive subglacial and/or ice-marginal drainage systems during deglaciation. This likely triggered asynchronous, and ice-stream bounded episodes of ice margin retreat, stillstands, and re-advances, which largely hinder efforts to correlate ice-marginal belts along the ice sheet and to date them as distinct phases of glaciation/deglaciation, i.e. discrete time intervals.

1. Introduction

Geomorphological record of the palaeo-ice margin positions is a robust proxy for reconstructing past ice sheets and their reaction to climate oscillations at the Last Glacial Termination, which occurred in the northern hemisphere about 20–7 ka (Denton et al., 2010; Cuzzone et al., 2016). Coupling geomorphological imprints of ice sheet dynamics to a time-scale, enables a better understanding of the ice margin fluctuations during the last deglaciation. It usually shows complex behavior with episodes of stillstands, local re-advances and/or extensive retreat. In addition, dynamics of the ice margin along peripheries of the continental ice sheets has been typically highly diversified, with asynchronous re-advances and retreats even in relatively close proximity to each other (Patton et al., 2013; Larsen et al., 2016; Kelley et al., 2018; Tylmann et al., 2022). After the Last Glacial Maximum (LGM), the general retreat of the southern Fennoscandian Ice Sheet (FIS) was discontinuous and non-linear (e.g., Marks, 2015; Hughes et al., 2016; Winsborrow et al., 2023). Various sectors of the palaeo-ice margin reacted differently, as they were potentially fed by independent palaeo-ice streams (e.g., Punkari, 1997; Boulton et al, 2001; Kalm et al., 2012; Roman, 2019; Lüthgens et al., 2020; Szuman et al., 2021; Tylmann et al., 2022). Moreover, climatic gradient which occurred along the southern margin of the last FIS, could have played an important role in differing dynamics between its western and eastern sectors (e.g., Larsen et al., 2016; Tylmann et al., 2022). Discontinuous character of the last deglaciation is recorded in the geomorphology of the FIS's peripheries as a distinct ice-marginal belts, i.e. assemblages of ice-marginal landforms, such as: terminal moraines, ice-marginal valleys, outlets of tunnel channels or proximal edges of outwash fans and outwash plains. However, because of asynchronous dynamics of the last FIS, the formation of ice-marginal belts was often time-transgressive, a pattern that might be manifested by motley geochronological results obtained from particular assemblages of ice-marginal landforms (Lüthgens et al., 2020; Tylmann et al., 2022).

In north-central Europe three main ice-marginal belts have been mapped, and traditionally ascribed to the three main phases of the last deglaciation: Brandenburg, Frankfurt, and Pomeranian Phases (Woldstedt, 1925, 1935; Fig. 1A). The Brandenburg (Leszno) Phase, dated at ~24–23 ka, is related to the local LGM in Germany and western Poland, and the Frankfurt (Poznań) Phase, dated at ~19 ka, is related to the local LGM in north-central and north-eastern Poland (Wysota et al., 2009; Marks, 2012; Tylmann et al., 2019, 2024; Krauß et al., 2025). The subsequent phases are correlated to the discontinuous retreat of the last FIS following the local LGM, among which the Pomeranian ice-marginal belt is the most prominent. However, besides these three main ice-marginal formations (Brandenburg, Frankfurt and Pomeranian), several minor ice margin fluctuations have been interpreted from geomorphological record in northern Poland (Kozarski, 1995; Niewiarowski et al., 1995; Mojski, 2005). One of the last fluctuation which occurred on the northern fringe of Poland left a distinct ice-marginal landsystem consisting conspicuous terminal moraines located in the vicinity of Lake Kopań, Lake Gardno and Lake Łebsko in the Polish middle-coast area (Fig. 1B, C). The Gardno moraines are clearly defined in the landscape, recording the ice margin position, probably after a local ice sheet re-advance of the so-called Gardno Phase during the general retreat dynamics of the last deglaciation (e.g., Bülow, 1924; Giedrojć-Juraha, 1949;

Sylwestrzak, 1978; Petelski, 1985; Kozarski, 1995; Rotnicki and Borówka, 1994, 1995; Jasiewicz, 1999).

Despite the growing number of geochronological data constraining the last FIS in northern Poland (e.g., Roman, 2019; Tylmann et al., 2019; 2022, 2024; Uścinowicz et al., 2019; Rychel et al., 2022; Tylmann and Uścinowicz, 2022; Kalińska et al., 2025), there is no direct numerical dating of ice-marginal landforms recording the last glacial episode in the present territory of Poland. Therefore, dynamics and chronology of the last FIS during the Gardno Phase remains elusive and questions related to the ice-margin positions along the northern fringe of Poland remains open. In particular, the question of the ice re-advance synchronicity between particular ice-marginal landsystems or the independence and asynchronicity between ice lobes re-advances is of much importance. A correlated issue is whether the ice re-advance during the Gardno Phase was local and constrained spatially only to the Polish middle-coast area, or if it could have been linked to ice re-advances recorded in the surrounding regions (northern Germany, southern Sweden, Baltic States?). Geomorphological and geochronological record of the Gardno Phase is one of the least recognized among the ice margin limits in the southern sector of the last FIS (Stroeven et al., 2016), with no detailed analyses of the glacial landforms based on digital elevation data and no direct dating of moraines with cosmogenic nuclides. Filling these gaps could potentially make a significant contribution to the discussion about the reliability of spatio-temporal correlation of marginal zones of the southern sector of the last FIS, and to the dating of these features as distinct phases of glaciation or deglaciation.

The aim of this paper is to reconstruct the main ice-marginal positions, local ice flow directions and timing of the ice margin oscillations during the last deglaciation on the northern fringe of Poland, based on geomorphology and ^{10}Be surface exposure ages. We use the approach of integrating detailed landforms analysis with cosmogenic surface exposure dating as one of the best way to understand the dynamics of the palaeo-ice sheet in details and deliver significant empirical data for further paleoclimatic reconstructions and numerical modelling. Here, we present new results of glacial landforms mapping and analysis based on high-resolution Digital Elevation Model (DEM) as well as ^{10}Be surface exposure dating of erratic boulders of the northern fringe of Poland. We then explore dynamics of the southern FIS front and timing of its fluctuations during one of the last Pleistocene glacial episode in the Polish Lowland.

2. Study area

The study area is located in the northern part of Poland, close to the coast of the Baltic Sea (Fig. 1A). It covers a region where ice-marginal landforms correlated with the Gardno Phase of the last deglaciation occur. The area stretches along the Baltic coast for a distance of ca. 130 km, from the vicinity of Lake Kopań in the west to the vicinity of Lake Żarnowieckie in the east. It consists of a few physiographic regions, such as: the Słowińskie Coast, northern edges of the Słupsk Plain and the Damnicka Plateau, the Żarnowiecka Plateau, and the northern part of the Kashubian Coast (Fig. 1B). The Gardno Phase is described in the literature as the last glacial episode in the present land territory of Poland. Timing of this episode was first proposed by Kozarski (1986) at 13.2 ka BP, based on: (1) uncalibrated radiocarbon ages of

organic deposits found beneath the LGM till in northern Poland (Pazdur, Walanus, 1979; Stankowska, Stankowski, 1979), (2) the average retreat rate of the last FIS following the local LGM in northern Poland, and (3) the correlation of the Gardno moraines in the central Polish coast with the so-called Low Baltic Stadial (Mörner et al., 1977). The first geochronometric dating of the Gardno moraines was made possible by uncalibrated radiocarbon ages obtained from the Łeba Barrier and the Łupawa alluvial fan (Fig. 1), which constrained the ice re-advance during the Gardno Phase to 14.5–14.3 ka BP (Rotnicki and Borówka, 1994; Kozarski, 1995). Subsequently, calibrated radiocarbon ages indicated a possible time window for this glacial phase between 16.8 and 16.6 cal ka BP (Marks et al., 2016), while OSL dating estimated it to fall between 16.0 and 15.5 ka (Uścinowicz et al., 2019). Recently, Tylmann and Uścinowicz (2022), based on Bayesian age modeling of available geochronological data (^{14}C, OSL), showed that the most likely age of the Gardno Phase is 16.5 ± 0.5 ka.

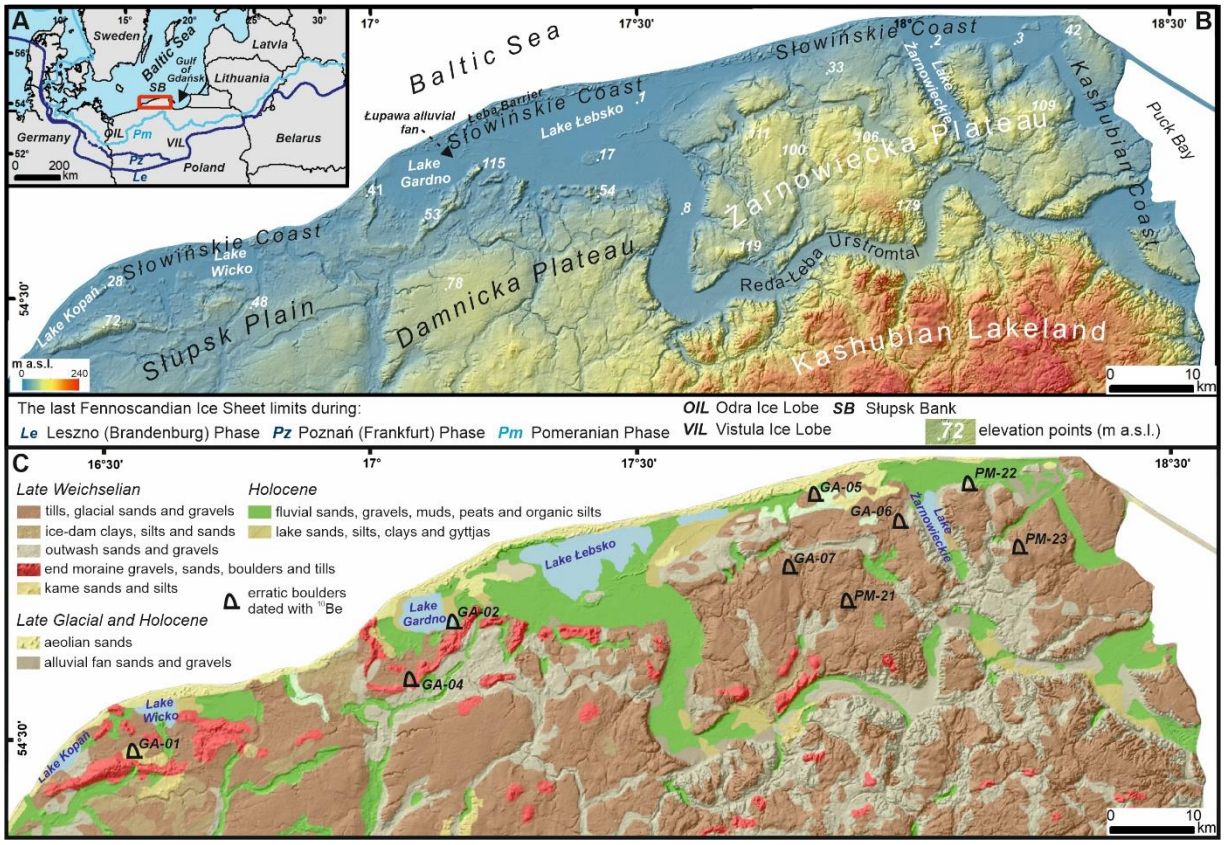

Fig. 1. Study area and location of large erratic boulders used in this study. (A) Location of the study area against the main limits of the last Fennoscandian Ice Sheet (FIS) and the main phases of the last deglaciation in north-central Europe. (B) Digital elevation model (DEM) of the study area with the main physiographic regions and selected elevation points. (C) Surface lithology of the study area based on Geological Map of Poland, 1:500 000 (Marks et al., 2006). Erratic boulders sampled for ^{10}Be surface exposure dating are also indicated.

The area of glacial landform analysis is located to the north of the Słupsk Plain, the Damnicka Plateau and the Reda-Łeba Urstromtal (ice-marginal spillway), where the assemblage of the Gardno ice-marginal landforms extending from west to east occur. Terrain elevation varies between ~sea level and 179 m a.s.l. The lowest elevations (around sea level)

occur in the Słowińskie Coast region along the coastline, and the highest elevations (>170 m a.s.l.) occur in the southern part of the Żarnowiecka Plateau. Most of the analyzed area is characterized by elevation ranging between around zero and 100 m a.s.l. The general trend in hypsometry shows the terrain inclination northward and westward. Local denivelations of the relief are up to 65-110 m and they occur between deeply incised valleys and highly elevated moraine plateaus or terminal moraines, particularly in the eastern part of the study area (Fig. 1B).

Glacial deposits dominate the surface geology of the study area, which is composed of upper Weichselian tills, boulders, gravel, sands, silts and clays (Fig. 1C). Tills, boulders and gravels are associated with either moraine plateau or end moraines. Sands occur in the areas of moraine plateau, end moraines, kames or former ice-dam lakes, while silts and clays are associated with the areas of kames and former ice-dam lakes. Outwash sands and gravels occur in the regions of glacial meltwater outflow, which in the study area are rather small spatially confined outwash plains. In addition, the Late Glacial and Holocene aeolian sands occur mainly along the coastline, where alluvial fan sands and gravels can also be locally found. Holocene deposits, such as fluvial sands, gravels, muds and lake sands, silts, clays, gyttjas together with peats and organic silts, occur mainly in glacial channels, river valleys and/or kettle holes and lake depressions (Fig. 1C). Surface geology of the study area is dominated by glacial deposits which makes the region relatively rich in large erratic boulders resting on the terrain surface.

3. Materials and methods

3.1. Landforms mapping

Glacial landforms were identified based on high-resolution DEM. We used DEM produced by laser scanning of the terrain surface (LiDAR – light detection and ranging) freely available from the geoportal.gov.pl database as 1-m grid tiles (last access: 15th of January 2025). Data were imported to ArcGIS Desktop 10.8.2 and were mosaiced to one raster file. The DEM was then converted to hillshade model with a NW illumination (azimuth 315° and altitude 45°) and an exaggeration (z factor) of 10. Landforms were mapped on-screen in ArcMap, at various scales (depending on landform size), by digitizing crest-lines of hills, upper slope breaklines of valleys and extent of landforms area to *shape* files, based on elevation and hillshade models. Additionally, information about surface lithology from detailed geological maps (1:50 000) available as WMS (Web Map Service) layers at the Polish Geological Institute-National Research Institute (baza.pgi.gov.pl/geoportal/uslugi/gis; last access: 15th of January 2025) were used in order to properly interpret type of landforms which were mapped. We identified nine types of glacial landforms that we define more thoroughly in the next paragraph: (1) moraine ridges, (2) subglacial lineations, (3) overridden moraines, (4) eskers, (5) kames, (6) hummocky moraines, (7) subglacial valleys, (8) subglacial meltwater corridors (SMCs), and (9) ice-marginal valleys.

Moraine ridges, overridden moraines, subglacial lineations and eskers were mapped as polylines by digitizing the crests of the landforms. Moraine ridges are ice-marginal landforms such as end/terminal moraines, which are traces of the former ice margin positions. Overridden moraines are moraine ridges, which were modified subglacially, they occur in the vicinity of

subglacial lineations and reveal streamlined morphology, often with arcuate shape bent in the direction of the ice flow (Fig. 2A). Subglacial lineations were identified as elongated, streamlined landforms parallel to each other and to the ice flow direction, up to several kilometer-long and gently emerging from the relief (e.g., Spagnolo et al., 2014). Eskers were mapped as elongated, curved ridges, composed of sand and gravel and expressing the positive morphological traces of subglacial channels.

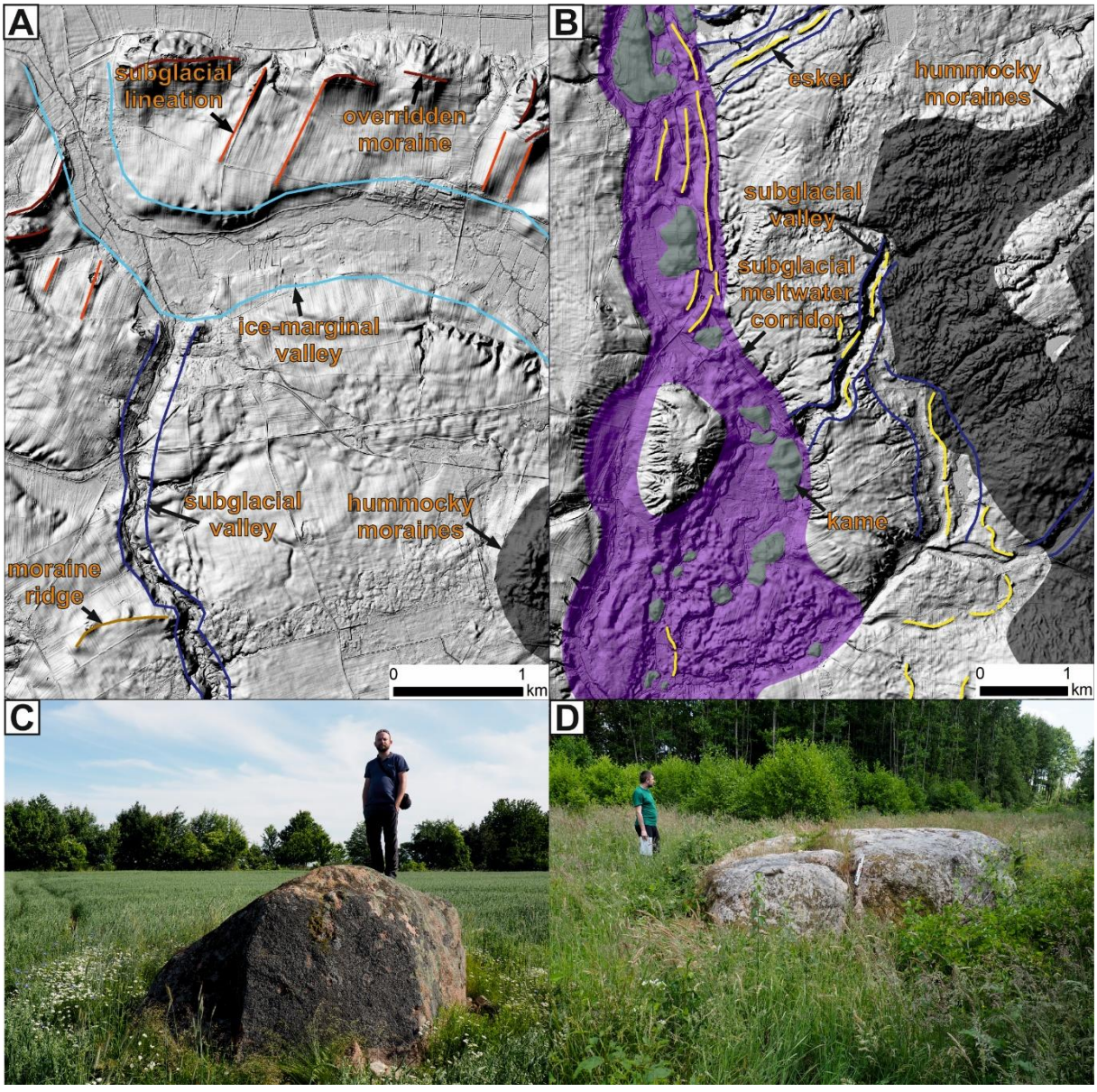

Fig. 2. Examples of mapped glacial landforms and erratic boulders sampled for ^{10}Be dating. (A) Moraine ridges, overridden moraines, subglacial lineations, hummocky moraines, subglacial and ice-marginal valleys. (B) Eskers, kames and subglacial meltwater corridors (SMCs). (C) Erratic boulder 1.7 m high, located on the surface of a moraine plateau. (D) Erratic boulder 1.0 m high, located within a subglacial valley.

Kames were mapped as polygons by digitizing their lower break-of-slopes, i.e. the base of the landforms. Areas of hummocky moraines with extremely irregular topography were mapped as polygons by digitizing the spatial extent of the hummocky-like topography. The

distinction between kames and hummocky moraines has been made and distinct individual landforms with kame-like morphology and lithology were mapped as individual kames, while areas of uncontrolled topography with numerous, connected and overlapping hummocks composed of glacial till, silt and gravel/sand were mapped as zones of hummocky moraines (Fig. 2B).

Subglacial valleys and ice-marginal valleys were mapped as polylines by digitizing their upper slope breaklines (Fig. 2A), while SMCs, which are much more extensive and have more diffused boundaries, were mapped as polygons representing the most likely extent of the subglacial meltwater routes (Fig. 2B). Subglacial valleys are morphological traces of concentrated, channelized subglacial meltwater erosion (subglacial channels) with distinct, linear morphology, rather narrow shape, abrupt start and end, undulated thalweg, and mostly parallel orientation to other subglacial features (lineations) and perpendicular to the former ice margin (e.g., Kehew et al., 2012). SMCs, on the other hand, represent broad, extensive zones of more diversified subglacial drainage with channelized and distributed water flow, erosion and deposition of sediments (e.g., Lewington et al., 2020). Their morphology is much more diffuse, less defined and usually more complex than subglacial valleys, consisting both of erosional features (channels, valleys) and of depositional features such as eskers and/or kames (Fig. 2B). Ice-marginal valleys were identified as tracks of mostly westwards ice-marginal meltwater outflow, usually perpendicular to subglacial valleys and subglacial lineations and parallel to the former ice margin, i.e. also to moraine ridges (e.g., Greenwood et al., 2007).

3.2. ^{10}Be surface exposure dating

For ^{10}Be surface exposure dating we chose boulders located on landforms associated with the potential limits of the ice sheet in the area of the northern fringe of Poland. Sampled boulders were large (perimeter >5 m) granitic rocks protruding above the ground surface. We sampled nine boulders (Table 1) located along the ice margin – from the vicinity of Lake Kopań in the west to the vicinity of Lake Żarnowieckie in the east (Fig. 1C).

Samples were taken with a manual jackhammer (PM samples) and hammer with chisel (GA samples) from the upper surface of nine boulders of perimeter ranging from 6.5 to 20.5 m (Table 1; Fig. S2 in Supplementary Materials). All boulders are characterized by quartz-rich lithologies as granitoids, granite gneisses and gneisses, and significantly protrude above the ground surface (height above ground ranging from 0.8 to 2.7 m) (Fig. 2C, D). Rock slabs of thickness from 1.0 to 3.2 cm were subjected to sample preparation which was conducted at the Laboratoire National des Nucléides Cosmogéniques at CEREGE, Aix-en-Provence, France for PM samples, and at the laboratory of the University of Gdańsk, Poland and at the CALM laboratory (Cosmonucléides Au Laboratoire de Meudon) at the Laboratoire de Géographie Physique (LGP), France for GA samples.

All samples were crushed and sieved. For PM samples, the 0.25–1.0 mm fraction was separated with a Frantz magnetic barrier laboratory separator in magnetic and non-magnetic subsamples. Several successive acid attacks of the non-magnetic fractions were performed using a mixture of concentrated hydrochloric acid (HCl) and fluorosilicic acid (H_2SiF_6). The purified quartz was decontaminated from meteoric ^{10}Be by three successive partial dissolutions

with concentrated hydrofluoric acid (HF). For GA samples, the 0.25-0.71 mm quartz fraction was separated by heavy liquid (sodium polytungstate) separation (to remove heavy minerals) and froth flotation (to remove feldspars). Several acid etchings (2% HF + HNO_3) in a hot ultrasonic bath were applied in order to purify the quartz. For all samples (PM and GA) the quartz purity was checked by ICP-OES analysis for Al content.

Purified quartz of PM samples was dissolved with concentrated HF after adding 100 µL of an home-made ^{9}Be carrier solution ([^{9}Be] = 3025 ± 9 µg/g, Merchel et al., 2008). Beryllium was recovered after two successive separations on ion exchange columns: an anion exchange column (Dowex 1X8) to remove iron and a cation exchange column (Dowex 50WX8) to discard boron and recover Be (Merchel and Herpers, 1999). The eluted Be fractions were precipitated to $Be(OH)_2$ with ammonia and oxidized to BeO. For GA samples the purified quartz was spiked systematically with ~460 mg of a commercial ^{9}Be carrier solution (concentration of 998 mg/l ± 3.7 mg/l) and then dissolved with concentrated HF. Beryllium was separated from remaining metals and purified in three stages: (1) anion column to remove Fe(III), (2) cation column to remove Ti, alkalis and separate Be from Al, and (3) hydroxide precipitation to remove residual alkalis, Mg and Ca. Then, $Be(OH)_2$ was oxidized to BeO.

For all samples (PM and GA) the BeO was mixed with niobium powder before being pressed in cathodes for accelerator mass spectrometry (AMS) measurements of the $^{10}Be/^{9}Be$ ratios at the French National AMS Facility ASTER, Aix-en-Provence (Arnold et al., 2010). The measured $^{10}Be/^{9}Be$ ratios were normalized relative to the in-house standard STD-11 using an assigned $^{10}Be/^{9}Be$ ratio of $(1.191 \pm 0.013) \times 10^{-11}$ (Braucher et al., 2015) and a ^{10}Be half-life of $(1.387 \pm 0.012) \times 10^{6}$ years (Chmeleff et al., 2010; Korschinek et al., 2010). Analytical 1σ uncertainties include uncertainties in AMS counting statistics, uncertainty in the standard $^{10}Be/^{9}Be$, an external AMS error of 0.5% (Arnold et al., 2010), and a chemical blank measurement ($^{10}Be/^{9}Be$ blank ratios for the GA batch is 6.57×10^{-15} and for the PM batch is 4.44×10^{-15}).

^{10}Be surface exposure ages were calculated using the most recent global production rate (Borchers et al., 2016) and the time dependent scaling scheme for spallation according to Lal (1991) and Stone (2000) (the 'Lm' scaling scheme). We corrected the ^{10}Be production rate for sample thickness according to an exponential function (Lal, 1991) and assuming an average density of 2.7 g/cm^3 for granitoid, granite gneiss and gneiss. An appropriate correction for self-shielding (boulder geometry) was applied when the surface of the sampled boulder had a slope of more than 10°. No correction for surface erosion of boulders was applied, as we interpret the ^{10}Be results as minimum surface exposure ages. All calculations were performed using the online exposure age calculator formerly known as the CRONUS-Earth online exposure age calculator – version 3 (http://hess.ess.washington.edu/math/; last access: 15th of January 2025), which is an updated version of the online calculator described by (Balco et al., 2008). Ages are reported with 1σ uncertainties (including analytical uncertainties and the production rate uncertainty).

4. Results

4.1. Landforms

A total number of 715 glacial landforms were mapped, including: 274 moraine ridges, 68 subglacial lineations, 74 overridden moraines, 52 eskers, 169 kames, 14 zones of hummocky moraines, 47 subglacial valleys, 5 SMCs, and 12 ice-marginal valleys (Fig. 3A, B).

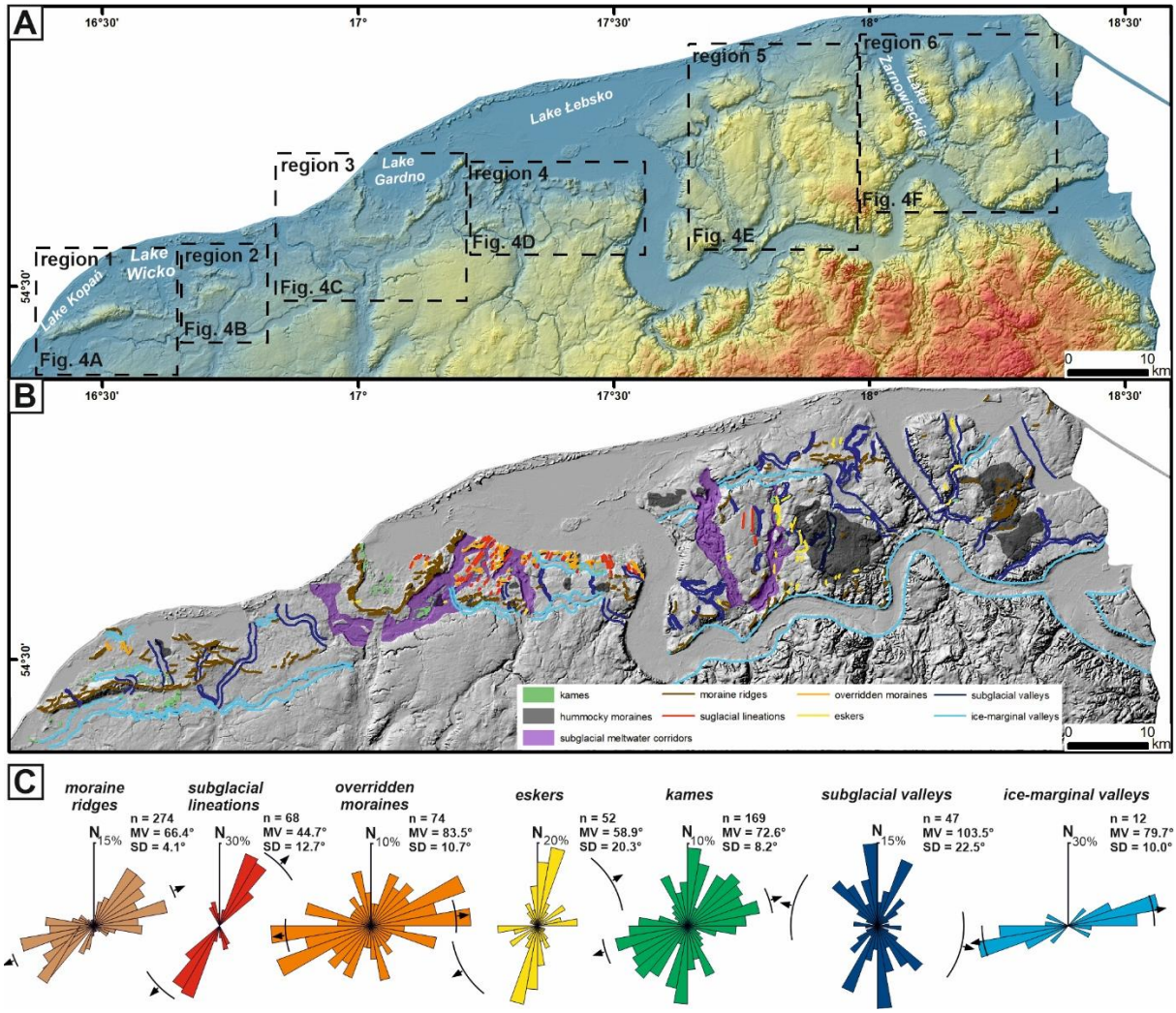

Fig. 3. Glacial landforms of the study area and their orientation. (A) Elevation and hillshade model for the study area. Black boxes represent regions shown in detail in figure 4 and described in the text. (B) Glacial landforms mapped along the northern fringe of Poland. The high-resolution map with delineated landforms is available in Supplementary Materials – Fig. S1. (C) Orientations of the long axes of mapped landforms shown as rose diagrams with basic statistical parameters: n – number of measurements, MV – mean vector, SD – standard deviation.

Moraine ridges occur throughout the analyzed area, from the southern surroundings of Lake Kopań to the west, east and south-east of Lake Żarnowieckie (Fig. 2B). They have mostly NE-SW and NEE-SWW alignments, but some ridges display diversified orientations recording lobated shapes of the ice margin (Fig. 3B, C). Subglacial lineations are oriented mainly NE-SW with small fractions of them oriented NW-SE (Fig. 3C). Overridden moraines occur in the vicinity of subglacial lineations in the central part of the study area (Fig. 3B). They have mostly E-W and ENE-WSW orientations (landforms generally transverse to the former ice flow) and

streamlined morphology with shape bent and smoothed southwards. Eskers are characterized by variable orientation, they are often aligned parallel to the subglacial valleys, with most of them oriented NNE-SSW (Fig. 3C). Kames have usually random orientation, with some oriented parallel to the subglacial channels and SMCs in which they occasionally occur.

Subglacial valleys run mostly N-S with some deviations in the eastward and westward directions, and only few single valleys are oriented west-east (Fig. 3C). Altogether, their orientation is rather variable. Subglacial valleys occur across the entire study area, dissecting moraine plateau, streamlined bedforms, hummocky moraines and/or moraine ridges. SMCs reveal convergent spatial orientation, with two corridors running NW-SE and NE-SW, and two corridors running NNW-SSE and NNE-SSW (Fig. 3B). Ice-marginal valleys run from east to west, they are usually parallel the moraine ridges, and they record palaeo-ice margin positions (Fig. 3B).

4.2. Landform associations

Landform associations occurring in the study area consist of subglacial, ice-marginal, proglacial and dead-ice topography formed during the general retreat of the last FIS. Traces of the ice margin positions are mostly moraine ridges (end moraines and terminal moraines) with ice-marginal valleys. They are often associated with outlets of subglacial valleys and SMCs, and/or proximal edges of outwash plains (Fig. 4A-F). Diverse morphologic relations between subglacial valleys and moraine ridges were identified: usually subglacial valleys terminate at the moraine ridges, however in some places they cross-cut moraines and terminate as ice-marginal valleys (Fig. 4A, B and D). Subglacial and ice-marginal valleys are incised in the surface of morainic plateaus and/or outwash plains, similarly to SMCs (Fig. 4E and F). However, SMCs are more extensive, their boundaries of are less clear and other landforms such as kames and eskers occur within them (Fig. 4C, D and E). This makes their relief very complex, with numerous hillocks, incisions and depressions occurring within them (Fig. 5A). Kames and eskers were also found within subglacial valleys (Fig. 4A, E and F). Both, subglacial valleys and SMCs cut morainic surfaces with subglacial lineations and overridden moraines, as well as with ice-marginal valleys (Figs. 4D, 5B). In some locations, ice-marginal valleys cut subglacial valleys and SMCs (Fig. 5A and C), while zones of hummocky moraines enter these valleys and corridors (Fig. 5A and D).

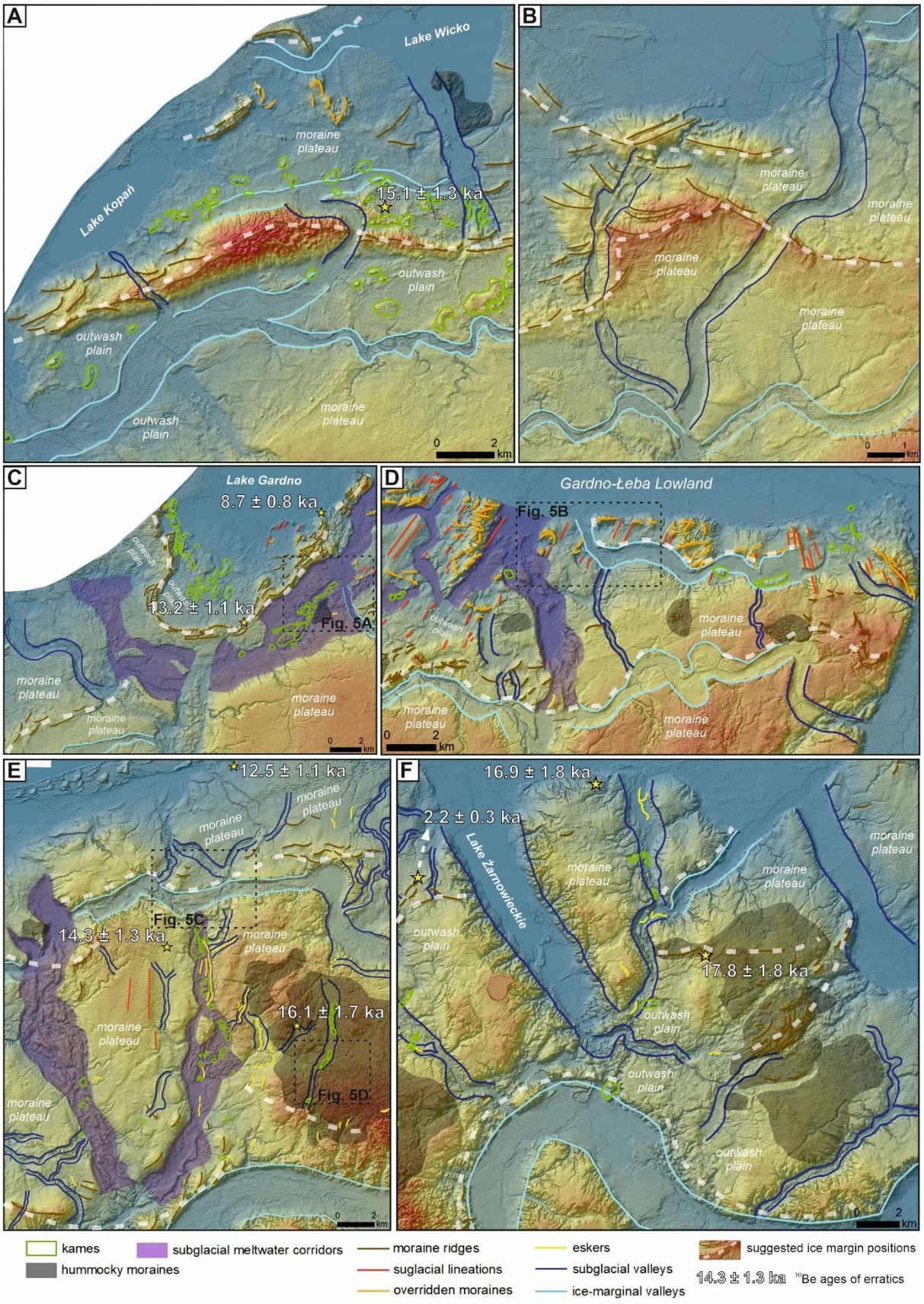

Fig. 4. Glacial landforms mapped in the study area and results of surface exposure ^{10}Be dating of erratic boulders. (A) Region 1: moraine ridges, overridden moraines, kames, subglacial and ice-marginal valleys mapped to the south of Lake Kopań and Lake Wicko. The prominent terminal moraines zone with outlet of subglacial valley and outwash plains with ice-marginal valleys on the foreland clearly

indicate ice margin positions. Two subglacial valleys cross-cut the terminal moraine zone. ^{10}Be surface exposure age of boulder located in between kames, close to the end moraine zone is indicated. (B) Region 2 : zone of moraine ridges, subglacial and ice-marginal valleys. One subglacial valley cross-cuts end moraines zone, while another one does not. Two ice-margin positions were identified. (C) Region 3: associations of landforms originated during the ice sheet retreat and re-advance around Lake Gardno. Two ice margin positions were identified. ^{10}Be surface exposure ages of boulders located along the lobate-shaped end moraines are indicated. (D) Region 4: glacial landforms mapped in the area to the east of Lake Gardno. Two ice margin positions and various glacial landforms cross-cutting each other were identified. (E) Region 5: associations of glacial landforms in the area south and south-east of Lake Łebsko. At least two ice margin positions were identified. ^{10}Be surface exposure ages of boulders located in central and northern part of the area are indicated. (F) Region 6: landsystem with subglacial valleys, eskers, moraines ridges, ice-marginal valleys, hummocky moraines and kames were mapped. ^{10}Be surface exposure ages of boulders located in central and northern part of the area are indicated.

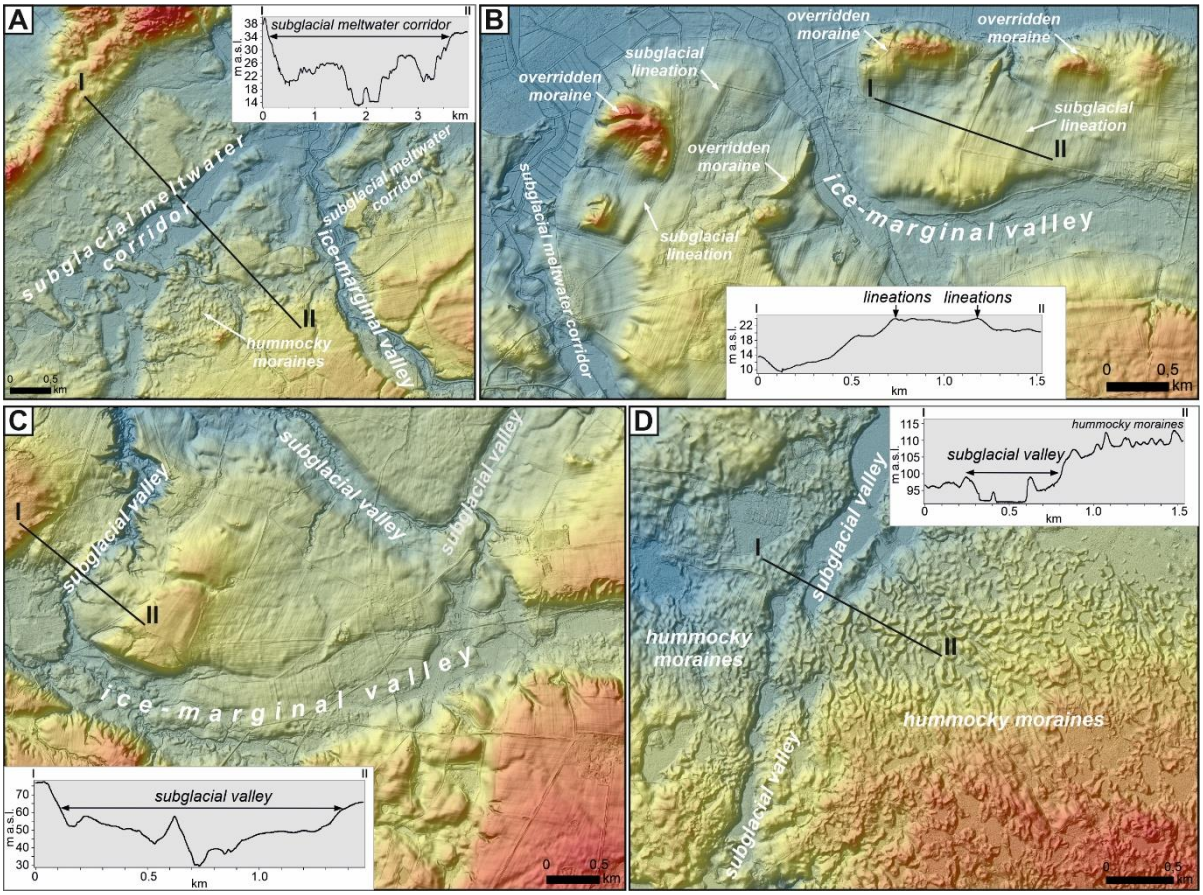

Fig. 5. Selected landforms associations occurring in the study area. (A) One of two SMCs occurring to the south of the lake Gardno. Note the complex topography of the SMC (morphological profile) and ice-marginal valley entering SMC. (B) Subglacial lineations and overridden moraines occurring east of lake Gardno. Note the low relief of the lineations (~1 m) and arcuate, streamlined morphology of overridden moraines. Both subglacial and ice-marginal valleys are cross-cutting subglacial lineations and overridden moraines. (C) Ice-marginal valley cross-cutting subglacial valleys. (D) Subglacial valley in the area of hummocky moraines. Note that hummocky moraines enter into the subglacial valley.

4.3. ^{10}Be surface exposure ages

^{10}Be ages of boulders range between 2.2 ± 0.3 ka and 17.8 ± 1.8 ka (Table 1). However, the ages between 12.5 ± 1.1 ka and 17.8 ± 1.8 ka overlap each other within the uncertainty range (Fig. 6). Ages 2.2 ± 0.3 ka and 8.7 ± 0.8 ka deviate the most from the other ages, they do not overlap within the uncertainty with other ages, and they are treated as outliers based on

statistical distribution. The ages between 12.5 ± 1.1 ka and 17.8 ± 1.8 ka also fall into a confidence interval arithmetic average ± 1.5 × IQR (interquartile range, which is the range between the third quartile – Q3 and the first quartile – Q1 of the population). Variability of the ages falling into the confidence interval (11.8%) slightly exceeds the average analytical uncertainty (9.3%), suggesting that the random uncertainties are dominated by geological/geomorphological uncertainties rather than by analytical ones.

Table 1. Erratic boulders used in ^{10}Be surface exposure dating. ^{10}Be ages calculated with the "Lm" time-dependent scaling scheme for spallation, according to Lal (1991) and Stone (2001) and the global production rate according to Borchers et al. (2016).

Boulder	Location [dd]		Dimensions [m]		Elevation [m a.s.l.]	Geomorphology	Sample thickness [cm]	Shielding factor[1]	Quartz [g]	^{10}Be [10^4 at g^{-1}]	Age [ka]
	Latitude N	Longitude E	Perimeter	Height							
GA-01	54.486	16.598	10.0	1.2	16	kame	1.0	1.00000	19.9453	6.429 ± 0.227	15.1 ± 1.3
GA-02	54.639	17.166	10.3	1.0	3	foothill of the moraine	3.1	0.98841	19.9240	3.578 ± 0.209	8.7 ± 0.8*
GA-04	54.575	17.092	6.5	0.8	27	foothill of the moraine	1.6	1.00000	20.0660	5.698 ± 0.217	13.2 ± 1.1
GA-05	54.794	17.844	11.5	1.2	12	subglacial valley	1.1	1.00000	22.0379	5.309 ± 0.200	12.5 ± 1.1
GA-06	54.759	17.997	12.0	1.1	53	moraine plateau	1.1	1.00000	20.1580	0.968 ± 0.110	2.2 ± 0.3*
GA-07	54.704	17.789	10.0	1.7	83	moraine plateau	1.2	1.00000	11.0437	6.539 ± 0.332	14.3 ± 1.3
PM-21	54.666	17.901	16.0	1.7	97	hummocky moraine	1.2	1.00000	19.4965	7.479 ± 0.525	16.1 ± 1.7
PM-22	54.800	18.128	20.5	2.7	35	edge of moraine plateau	1.8	0.97743	19.7629	7.153 ± 0.540	16.9 ± 1.8
PM-23	54.728	18.211	13.4	2.4	103	terminal moraine	3.2	0.99936	15.3901	8.167 ± 0.549	17.8 ± 1.8

[1] corresponding to self-shielding (direction and angle of surface dip)

* ages treated as outliers

The distribution of ^{10}Be ages plotted against the longitudinal position of the samples reveals that two ages from the western part of the study area that fall into a confidence interval are 13.2 ± 1.1 ka and 15.1 ± 1.3 ka (Fig. 6). In the eastern part of the study area, the ages within the confidence interval range from 12.5 ± 1.1 ka and 17.8 ± 1.8 ka, with a mean age and standard deviation of 15.5 ± 1.9 ka (n = 5).

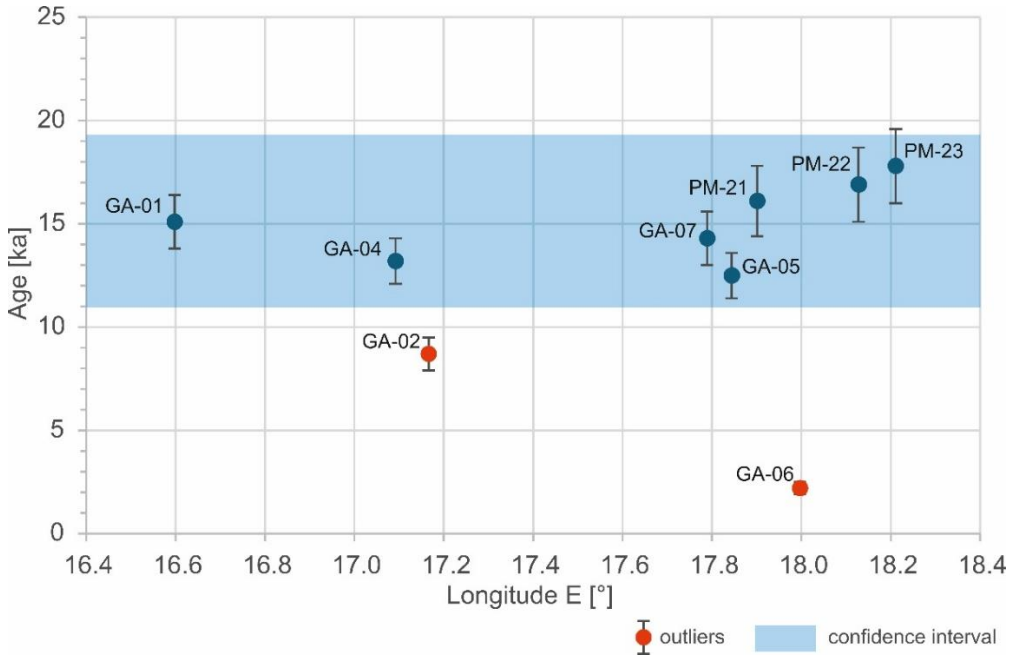

Fig. 6. Distribution of ^{10}Be ages plotted against the longitudinal location of sampled boulders.

5. Interpretation of landforms distribution and ^{10}Be surface exposure dating

5.1. Relative chronology

Relative chronology of glacial events might be inferred from spatial and elevation relations between landforms (e.g., Greenwood and Clark, 2009; Hughes et al., 2014; Kamleitner et al., 2024). South of Lake Kopań and Lake Wicko (region 1 in Fig. 3A) the ice sheet retreated and left kames in the landscape (ice sheet rich in crevasses?). Subsequently a main ice margin stillstand occurred when a prominent terminal moraine system was formed with two subglacial valleys dissecting moraine ridges with one terminating at the moraines (Fig. 4A). On the foreland of the moraines and subglacial valleys, small, confined outwash plains have been deposited, and proglacial meltwater running westwards eroded ice-marginal valleys. Subglacial valleys which cut moraine ridges were probably formed time-transgressively when the ice margin was positioned further north, while the subglacial valley which terminates at the moraine ridges (south of Lake Wicko) was probably formed during the main ice margin stillstand along the moraines. Following this episode, ice sheet retreated again leaving kames and moraine plateaus in the landscape, together with few recessional moraines and ice-marginal valleys indicating minor ice margin stillstands. Overridden moraines occurring to the north of the prominent terminal moraine system suggest that the main ice margin stillstand in this area might have occurred after the local ice re-advance (Fig. 4A). The relative chronology of glacial landforms in the landscape is the following: (1) kames located to the south of the main terminal moraines; (2) overridden moraines; (3) the main terminal moraines, subglacial valleys, outwash plains and ice-marginal valleys located to the south of the main moraines; (4) kames, ice-marginal valleys and moraine ridges located to the north of the main moraines; (5) hummocky moraines.

In region 2 (Fig. 3A), the ice sheet retreat has been punctuated by ice margin stillstands, which may be inferred from terminal moraine ridges and ice-marginal valleys occurring both on the foreland and in the hinterland of the moraines. Subglacial valleys have been eroded time-transgressively as the ice margin was retreating and terminating: on one hand, the western subglacial valley is cut by terminal moraine ridge, which means that the subglacial channelized drainage was inactive here at the time of ice margin stillstand and moraines deposition. On the other hand, the eastern subglacial valley cuts terminal moraine ridge, which means that subglacial drainage was probably continuously active as the ice margin was retreating and terminating (Fig. 4B). The relative chronology of glacial landforms in this region is the following: (1) ice-marginal valley located to the south of the terminal moraines and beginning of subglacial valleys incision, (2) the main terminal moraines and continuation of subglacial valleys incision, (3) moraine ridges located to the north of the main moraines; (4) ice-marginal valley located in the north-eastern corner of the area. The main terminal moraine ridges here are continuations of the prominent terminal moraine system to the west (Fig. 3A and B).

Two SMCs indicate broad zones of subglacial meltwater erosion and deposition to the south of Lake Gardno in region 3 (Fig. 3A). Orientations of the SMCs suggest convergent meltwater flow from NW to SE and from NE to SW. As the ice margin retreat was continuing, a system of terminal moraine ridges running SW-NE with NW-SE oriented subglacial valley

was formed in the western part of the area, and a NW-SE oriented ice-marginal valley cutting SMC was formed in the eastern part of the region (Figs. 4C and 5A). This suggests that two ice lobes with a convergent ice flow pattern occurred to the south of Lake Gardno, as the ice margin was retreating. Kames and hummocky moraines, which occur within the NE-SW oriented SMC, were formed during the retreat of the eastern lobe. The ice margin then re-advanced in a narrow zone of the present Lake Gardno, and formed a prominent, lobate-shaped moraine ridge. This landform is younger than the previous ones, and indicate a local, narrow ice re-advance, which may be also inferred from a few subglacial lineations and overridden moraines occurring to the south of Lake Gardno (Fig. 4C). Finally, kames located to the north of the prominent, lobate-shaped moraine ridges have been formed as a result of the final deglaciation. We suggest the following relative chronology of glacial landforms in this region: (1) SMCs, (2) kames and hummocky moraines occurring within SMC, (3) moraine ridges and the subglacial valley located in the western part of the area; (4) ice-marginal valley located in the eastern part of the area; (5) a few subglacial lineations with overridden moraines and lobate-shaped moraines ridges south of Lake Gardno; (6) kames located north of the lobate-shaped moraine ridges.

In region 4 (Fig. 3A), subglacial lineations and overridden moraines have been formed as a results of ice sheet overriding (probably the pre-existing moraine plateaus) and shaping of the ice bed, most likely by warm-based, active ice. A divergent ice flow pattern is recorded here by lineations oriented NE-SW in the western and central parts of the area and NW-SE in the eastern part (Fig. 4D). Subsequently, SMCs and subglacial valleys were formed, thus imprinting the surfaces with subglacial lineations (Fig. 5B). SMCs here are most likely part of the same system as the SMCs occurring south of Lake Gardno. As an ice margin stillstand occurred, the ice front was located along the ice-marginal valley and terminal moraine ridges running from east to west in the southern part of the area. This ice-marginal valley continues to the west and it corresponds to a valley which cuts through SMC in the eastern part of region 3 (Fig. 4C and D, Fig. 5A). Hummocky moraines have been deposited and another ice margin stillstand occurred during the ice sheet recession in the northern part of the region. The relative chronology of glacial landforms in this area is the following: (1) subglacial lineations and overridden moraines, (2) SMCs and subglacial valleys, (3) moraine ridges and ice-marginal valley located in the southern part of the area; (4) hummocky moraines, (5) ice-marginal valley located in the northern part of the area, (6) kames.

In region 5 (Fig. 3A) a gentle subglacial lineations occurring within the moraine plateau in the central part of the region and SMCs with subglacial valleys and eskers, indicate subglacial shaping of the ground moraine surface and subsequent (or simultaneous?) subglacial meltwater erosion and deposition occurring under the last ice sheet. The first ice margin stillstand during the ice sheet recession occurred along the terminal moraine ridges, ice-marginal valley and outlets of SMCs and subglacial valleys in the southern part of the area. The ice margin then retreated to the north, hummocky moraines and kames were formed, and younger ice margin stillstands occurred in the northern part of the area along moraine ridges, ice-marginal valley and outlets of subglacial valleys (Fig. 4D). The relative chronology of glacial landforms in this area is the following: (1) subglacial lineations, (2) SMCs, subglacial valleys and eskers connected to the southern ice margin positions, (3) terminal moraine ridges and ice-marginal

valley in the southern part of the area, (4) hummocky moraines and kames, (5) subglacial valleys and eskers connected to the northern ice margin positions (6) moraine ridges and ice-marginal valley located in the northern part of the area.

The last area where landform associations and relative chronology of glacial events were analyzed is region 6, located around Lake Żarnowieckie (Fig. 3A). A few possible ice margin stillstands occurring during the general ice sheet retreat have been identified there. The first stillstand occurred along the prominent ice-marginal valley and outlets of subglacial valleys in the southern part of the area. Two younger ice-margin stillstands are then recorded by moraine ridges located to the east and southeast of Lake Żarnowieckie. These stillstands are likely related to the outlet of the Lake Żarnowieckie subglacial valley and the formation of small confined outwash plains south of the valley (Fig. 4F). The Lake Żarnowieckie subglacial valley is a complex tunnel valley formed through repeated phases of subglacial meltwater erosion of the ice bed, followed by infilling with fluvioglacial and glaciolacustrine deposits. This process began as early as the Elsterian glaciation (MIS 12) and continued through the subsequent glacial–interglacial cycles (Błaszkiewicz and Tylmann, 2024). Evidence for this includes a wide (up to 4 km) and deep (up to 323 m b.s.l.) buried valley that dissects Cenozoic and Jurassic-Cretaceous sediments, and even reaches Triassic strata, following the axis of Lake Żarnowieckie (Małka et al., 2023). The tunnel valley underwent multiple episodes of dissection and burial, with the final shaping of the open valley visible in today's landscape occurring during the last deglaciation. The youngest stillstand which occurred in this area may be traced along moraine ridges and outlets of subglacial valleys to the west of Lake Żarnowieckie, and also along the ice-marginal valley to the east of Lake Żarnowieckie (Fig. 4F). We suggest the following relative chronology of glacial landforms in this region: (1) subglacial valleys connected to the southernmost ice margin positions, (2) the prominent ice-marginal valley in the southern part of the area, (3) moraine ridges located to the southeast of Lake Żarnowieckie; (4) hummocky moraines; (5) subglacial valleys connected to the northernmost ice margin positions; (6) moraine ridges and ice-marginal valley in the northern part of the area.

5.2. Timing of ice margin positions

As we present the exposure ages without erosion, snow-cover or vegetation-cover correction, we interpret them as minimum ages for the last deglaciation in the study area. Two ages (samples GA-02 and sample GA-06) are most likely influenced by postglacial erosion of boulder surfaces, exhumation of boulders from glacial deposits after deglaciation and/or anthropogenic activity. Boulder GA-02 (8.7 ± 0.8 ka) is located at the foothill of the moraine ridge, at the edge of Lake Gardno depression (Fig. S2B in Supplementary Materials), and it could have been released by a dead-ice block relatively long after deglaciation. The final melting of dead-ice blocks in northern Poland occurred even during the beginning of the Holocene, in the Preboreal chronozone ca. 11.2 cal ka BP (Słowiński et al., 2015). Boulder GA-06 (2.2 ± 0.3 ka) is located on the surface of the moraine plateau, but at the edge of a field, next to a paved road (Fig. S2E in Supplementary Materials). The anomalous young exposure age of this boulder is probably the result of human excavation.

In region 1, south of Lake Kopań and Lake Wicko, an erratic boulder located within the kame landscape, close to the prominent terminal moraine, was dated at 15.1 ± 1.3 ka (Fig. 4A and Fig. S2A in Supplementary Materials). Two erratics located on the prominent, lobate-shaped moraine ridges south of Lake Gardno in region 3, were dated at 8.7 ± 0.8 ka and 13.2 ± 1.1 ka (Fig. 4C). While we interpret the age of 8.7 ± 0.8 ka as an outlier, the age 13.2 ± 1.1 ka may indicate the minimum age of deglaciation. However, this exposure age is probably also "too young", due to boulder deposition from dead ice blocks and/or exhumation from morainic deposits after deglaciation, as it is located at the foothill of the moraine ridges (Fig. S2C in Supplementary Materials). In the area east and southeast of Lake Łebsko in region 5, three erratic boulders were dated at 12.5 ± 1.1 ka, 14.3 ± 1.3 ka and 16.1 ± 1.7 ka (Fig. 4E). While 14.3 ± 1.3 ka and 16.1 ± 1.7 ka (samples GA-7 and PM-21) seems to be reliable for a possible timing of deglaciation, the age of 12.5 ± 1.1 ka (sample GA-05) is probably "too young", also due to boulder deposition from dead ice blocks and/or exhumation from glacial deposits after deglaciation. Between 13.6 and 11.4 ka, the southern margin of the FIS deposited the Trollhättan, Levene, and Middle Swedish end moraine zones approximately 340–420 km north of the study area (Stroeven et al., 2016). Boulder GA-05 is located within the narrow, subglacial channel dissecting moraine plateau (Fig. S2D in Supplementary Material). Thus, there is a possibility, that the channel was infilled with dead ice after deglaciation, and/or the erratic was freed from sediments due to glaciofluvial/fluvial erosion along the channel.

Three erratics have been dated in region 5 around Lake Żarnowieckie, and their exposure ages are 2.2 ± 0.3 ka, 16.9 ± 1.8 ka and 17.8 ± 1.8 ka (Fig. 4F). While we interpret the age of 2.2 ± 0.3 ka as an outlier, ages 16.9 ± 1.8 ka and 17.8 ± 1.8 ka are probably reliable for the possible deglaciation timing, as supported by results just south of the study area from a recent paper by Tylmann et al. (2022).

Variability of the ^{10}Be ages indicates that geomorphological factors strongly influenced the apparent exposure ages in the study area. The detailed geomorphological location of each boulder is given in Table 1 and Fig. S2 in the Supplementary Materials. ^{10}Be ages which we interpret as reliable indicators for deglaciation timing (GA-01, GA-07 and PM samples), are located on kames, terminal moraines or moraine plateau. Whereas ^{10}Be ages which are evident outliers (GA-02 and GA-06) or are most likely "too young" (GA-04, and GA-05) are located mainly within the valleys/depressions and at the foothill of the moraines (Tab. 1) or eventually on the moraine plateau (GA-02), but in the locality where anthropogenic activity is very likely. This stresses the importance of proper geomorphological location of the sampled boulders in an ice sheet marginal context (top of hills, flat and stable morainic plains) for reliable surface exposure dating interpretation (Heyman et al., 2011; Tomkins et al., 2021).

6. Discussion

6.1. Ice margin oscillations and ice flow directions

Analysis of glacial landforms spatial distribution based on LiDAR DEM, supplemented with ^{10}Be surface exposure dating of erratics, provided us with the necessary information to reconstruct the last ice sheet dynamics and timing of ice margin fluctuations on the northern fringe of Poland. Relative chronology of glacial events inferred from spatial arrangement of

mapped landforms, suggests dynamic oscillations of the ice sheet with episodes of the ice margin retreat, stillstands and re-advances. The Gardno moraines, described in the literature as a distinct ice-marginal belt correlated with the last Pleistocene ice re-advance in the Polish Lowland (Kozarski, 1995; Rotnicki and Borówka, 1994, 1995; Marks, 2002), are in fact diversified ice-marginal landsystems representing discontinuous ice sheet retreat, and episodes of various ice lobes stillstands and/or re-advances. ^{10}Be surface exposure dating suggests asynchronous dynamics of particular ice streams/ice lobes across the study area (Fig. 7).

The earliest ice margin stillstand occurred in the eastern part of the study area, most likely no later than ~17.5 ka (average of two ^{10}Be ages 16.9 ± 1.8 ka and 17.8 ± 1.8 ka). Ice flow pattern was convergent with a direction of NE-SW according to the orientation of the subglacial valleys SE of Lake Żarnowieckie, and a direction of NW-SE along the subglacial valley SW of Lake Żarnowieckie (Fig. 7). The ice flow from NE to SW in the eastern edge of the study area is consistent with the general ice flow pattern within the western flank of the Vistula Ice Lobe (Marks et al., 2006; Marks, 2012). However, during the retreat of the ice margin to the north, the ice flow direction switched to a NW-NE pattern, which is indicated by subglacial valleys and moraine ridges occurring to the east of the Lake Żarnowieckie. These directions are consistent with fabric data obtained from till deposits representing the last ice advance and retreat in the areas around the Gulf of Gdańsk (Woźniak and Czubla, 2015). West of Lake Żarnowieckie the main ice margin stillstand occurred slightly later (Fig. 7). There the ice sheet retreat started most likely before ~15 ka (average of two ^{10}Be ages 14.3 ± 1.3 ka and 16.1 ± 1.7 ka). Two ice lobes had convergent ice flow pattern, based on the interpretation of subglacial valleys and moraine ridges orientation. Although the distance along the ice margin between the areas to the east and to the west of Lake Żarnowieckie is not significant (30–40 km), the main ice margin positions occurred at a different time (asynchrony), and the offset could be as much as ~1–2 ka. In the area south of Lake Łebsko, the main ice margin position could be a westward continuation of the ice lobes margin mentioned above (Fig. 7). However, there are no ^{10}Be ages which can constrain the timing of this ice margin position, we only know from the geomorphological relations, that it is older than the ice re-advance which formed the prominent arc of terminal moraines around Lake Gardno.

Along the western segment of the ice-marginal belt, the main ice margin stillstand occurred along the prominent terminal moraine to the south of Lake Kopań, most likely before ~15 ka (^{10}Be age 15.1 ± 1.3 ka). The ice flow direction was here mainly NNW-SSE (Fig. 7). The main ice margin position dated here is probably slightly younger than the ice margin position to the west of Lake Żarnowieckie, however this dating is inferred only from one ^{10}Be age and must be treated with caution. The main ice margin position in the area between Lake Kopań and the prominent arc of terminal moraines around Lake Gardno is probably the continuation of the one mentioned above. There are no ^{10}Be ages, however the geomorphological relations show clearly that it is older than the ice re-advance which formed moraines around Lake Gardno. The youngest glacial episode was the ice re-advance and formation of a prominent arc of terminal moraines south of Lake Gardno (Fig. 7). These moraines have strongly deformed structure with numerous glaciotectonic thrusts and scales (Jasiewicz, 1999). This indicates dynamic ice re-advance with thrusting and pushing of the ice

sheet foreland and formation of a lobate-shaped moraine system (Fig. 4C). The re-advance occurred within the local and narrow ice stream/ice lobe flowing from the NE. Our ^{10}Be dating can only constrain that the ice retreat after this re-advance occurred before ~13 ka. However, radiocarbon dates of organic deposits from Łeba Barrier and Łupawa alluvial fan overlying a till/boulder horizon and correlated with the re-advance (17.5 ± 0.2 cal ka BP and 16.8 ± 0.4 cal ka BP) suggest that it must have occurred much earlier than ~13 ka (Rotnicki and Borówka, 1994; Tylmann and Uścinowicz, 2022).

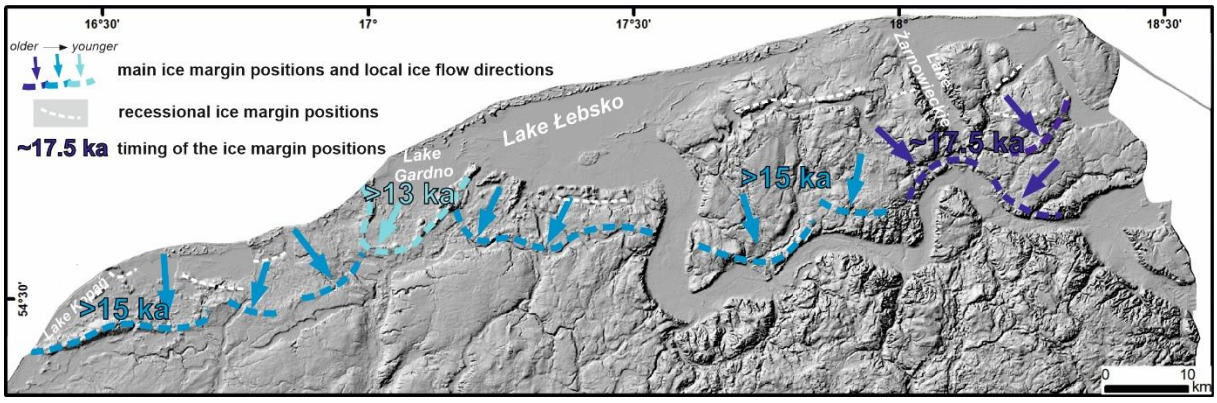

Fig. 7. Reconstruction of the last ice sheet on the northern fringe of Poland. The main ice margin positions are given together with local ice flow directions and timing inferred from ^{10}Be surface exposure dating. Recessional ice margin positions are also marked. Note the individual ice stream/ice lobes shaping the ice margin and variable timing for the ice margin positions.

Dynamic oscillations of the palaeo-ice margin on the northern fringe of Poland, characterized by frequent episodes of ice margin retreat, stillstands, and re-advances, may have been driven by the presence of large volumes of meltwater within the retreating ice sheet and the development of intensive subglacial and/or ice-marginal meltwater drainage systems. This inference is supported by the significant occurrence of meltwater-related glacial landforms and deposits identified in the study area, including SMCs, subglacial and ice-marginal valleys, eskers, and outwash plains. The presence of pressurized meltwater within the ice sheet can promote decoupling of the ice from its bed, leading to pronounced dynamic instability (e.g., Kjær et al., 2006; Storrar et al., 2014). Cycles of glacial surges, terminating in ice stagnation as pressurized meltwater is evacuated from the ice/bed system to the ice sheet foreland, may explain the highly dynamic oscillations of the ice margin (Hoffman and Price, 2014; Thøgersen et al., 2024). The significant role of meltwater activity in influencing the dynamic behavior of the retreating ice sheet and in the formation of spectacular glacial landforms has been previously proposed for various regions in northern Poland (e.g., Lesemann et al., 2010, 2014; Weckwerth et al., 2019; Hermanowski and Piotrowski, 2022).

6.2. Ice sheet dynamics and the "Gardno Phase"

The maximum extent of the last FIS was recently dated at ~24–23 ka during the Brandenburg (Leszno) Phase in Germany and western Poland (Ehlers et al., 2011; Marks, 2012; Tylmann et al., 2019; Krauß et al., 2025) and at ~19 ka during the Frankfurt (Poznań) Phase in north-central and north-eastern Poland (Wysota et al., 2009; Tylmann et al., 2019, 2024). After

its maximum extent, the FIS generally retreated with episodes of ice margin stillstands and/or re-advances. One of the main, regionally correlated, stage of this discontinuous retreat was the Pomeranian Phase – expressed in the landscape as a distinct ice-marginal belt running through Pomerania in northern Poland and northeastern Germany (Kłysz, 2003; Błaszkiewicz, 2011; Börner et al., 2019). Recently, Tylmann et al. (2022) proposed an asynchronous dynamics of the last FIS along the Pomeranian ice-marginal belt, with timing for the ice margin positions at ~19–18 ka for the Odra Ice Lobe, at ~20–19 ka in the interstream area between the Odra and the Vistula Ice Lobes and again at ~19–18 ka for the Vistula Ice Lobe. In the absence of any time constraints other than our single ^{10}Be exposure ages, the timing of the ice margin stillstand in the eastern part of the study area dated at ~17.5 ka seems plausible, when comparing it to the age of the Pomeranian ice-marginal belt in the Vistula Ice Lobe dated at ~18.5 ka (n = 3 ^{10}Be ages, Tylmann et al., 2022). This would indicate an average retreat rate of about 75 m/yr for the last FIS between the Pomeranian moraines and the ice margin position south of Lake Żarnowieckie, which is a possible retreat rate for land-terminating ice streams/ice lobes (e.g., Smedley et al., 2017; Bradwell et al., 2019). The younger age of the main ice margin positions (>15 ka) to the west of Lake Żarnowieckie and in the western part of the study area are also acceptable in the light of the age of the Pomeranian ice-marginal belt to the west of the Vistula Ice Lobe estimated at ~20–19 ka (Tylmann et al., 2022).

The ice margin stillstand of the last FIS, which occurred after the Gardno Phase is recorded in the glacial landforms mapped offshore – on the Słupsk Bank (Fig. 1A) in the southern Baltic (Uścinowicz, 1999, 2014). Timing of this stillstand was recently estimated based on Bayesian modeling of various geochronological data to around 15.5 ka (Tylmann and Uścinowicz, 2022). This means that the possible time window for the ice margin positions on land in the study area must pre-date this timing. Thus, the youngest segment of the main ice margin position in the area south of Lake Kopań (>15 ka), as well as the younger ice re-advance around Lake Gardno (>13 ka), are both older than ~15.5 ka. However, the precise dating of these ice margin positions based on our new data is not possible, and further numerical dating (OSL, ^{14}C) would be necessary. But we know that these ice margin segments are younger than ~20–19 ka and older than ~15.5 ka, and that the ice re-advance around Lake Gardno is younger than the ice margin stillstand south of Lake Kopań.

So far, the last FIS extent during the Gardno Phase in northern Poland has been reconstructed as a continuous marginal zone along the moraine ridges south of the Lake Kopań and Lake Wicko (Fig. 4A), along the moraine arc south of Lake Gardno (Fig. 4C) and along the morphological break between the moraine plateau and the Gardno-Łeba Lowland (Fig. 4D) further to the east (Rotnicki and Borówka, 1994, 1995; Kozarski, 1995; Mojski, 2005). The ice sheet limit correlated with the Gardno Phase in the eastern part of the study area (Żarnowiecka Plateau, Fig. 1) has been open to more controversy: some authors mapped this ice limit to the south of lake Żarnowieckie (Uścinowicz, 1999; Mojski, 2000), while others mapped the limit more to the north (Sylwestrzak, 1978; Kozarski, 1995; Marks, 2012). Our study illustrates that the main ice-marginal landsystems across the study area are composed of distinct ice lobes, and that timing for the particular ice streams/ice lobes was diverse from east to west and with rather older ice margin positions in the east than in the west (Fig. 7). During the ice sheet retreat, the

direction of the ice flow was shifting, especially in the eastern part of the study area, and episodes of the ice margin stillstands and/or re-advances occurred. The youngest ice re-advance formed the arcs of terminal moraines south of Lake Gardno – corresponding to the imprint on the landscape of a narrow (ca. 12 km) ice lobe, which was the basis for distinguishing the Gardno Phase as a morphostratigraphic unit in the past (e.g., Bülow, 1924; Giedrojć-Juraha, 1949; Sylwestrzak, 1978; Petelski, 1985; Kozarski, 1995; Rotnicki and Borówka, 1994, 1995; Jasiewicz, 1999). Any spatial correlation of this moraine arc with moraine ridges of possibly the same age is impeded, as the moraines were probably reshaped or simply destroyed during the Holocene transgression of the southern Baltic. Most likely, only remnants of these ridges may exist on the present seafloor, in the form of relict moraines and/or boulders fields (Uścinowicz, 1999; Tylmann and Uścinowicz, 2022).

6.3. Wider implications

The geomorphological signatures of the ice-margin positions along the frontal zone of this extensive palaeo-ice sheet constitute a cumulative record of ice fluctuations that varied both spatially and temporally. This study confirms the asynchronous and time-transgressive development of ice-marginal belts during the last deglaciation on the southern fringe of the last FIS (Larsen et al., 2016; Hughes et al., 2021; Tylmann et al., 2022). Distinct ice streams, which supplied ice to the marginal zones during the general retreat of the ice sheet following the LGM, controlled oscillations of the ice margins that could occur at different times, even in close proximity. These local ice retreats, stillstands, and re-advances were likely influenced primarily by local factors, such as internal ice dynamics, the topography of the ice foreland, and/or the rheology of the ice/bed interface. Additionally, the presence of large volumes of meltwater within the ice sheet and its drainage system was probably one of the most significant factors contributing to the highly dynamic and typically asynchronous oscillations of the ice margins along the ice sheet's periphery.

Dynamics of ice sheets and complex development of the ice-marginal formations during glacial cycles largely impede the correlation of individual ice-marginal belts and the dating of these features as distinct phases of glaciation or deglaciation, i.e. discrete time intervals (Tylmann et al., 2022). Ice advances and retreats were most likely locally constrained within numerous zones of consistent ice dynamics and chronology – namely, narrow and independent ice streams operating in the marginal sectors of the ice sheet (Greenwood et al., 2024). Consequently, any regional correlations of synchronous ice sheet limits along the southern margin of the last FIS (e.g., Uścinowicz, 1999; Mojski, 2000, 2005; Marks, 2012, 2015; Stroeven et al., 2016) are extremely difficult, if not entirely unfeasible. Instead, reconstructions and dating of local areas with relatively uniform ice stream dynamics and chronology are likely to be more reliable and subject to smaller sources of errors.

7. Conclusions

Analysis of the spatial distribution of glacial landforms using LiDAR DEM, supplemented by ^{10}Be surface exposure dating of erratics, has provided essential information for reconstructing the last ice sheet's dynamics and timing of ice margin fluctuations along the

northern fringe of Poland. The data provided supporting evidence to elucidate the dynamics and chronology of local ice margin fluctuations and to investigate one of the last glacial episodes in the present-day territory of Poland (the Gardno Phase). More importantly, the data point to the potential causes of ice margin dynamics and asynchrony, as well as acknowledge the challenges of establishing regional spatio-temporal correlations of ice sheet limits along the southern margin of the last FIS. Our results lead to the following conclusions:

- The last glacial episode in the present onshore territory of Poland was characterized by dynamic oscillations of the ice sheet with the ice margin retreats, stillstands and re-advances.
- Analysis of glacial landforms distribution supplemented with ^{10}Be surface exposure dating suggest asynchronous dynamics of particular ice streams/ice lobes across the northern fringe of Poland traditionally attributed to the Gardno Phase ice-marginal landforms.
- The main ice margin positions on the northern fringe of Poland were dated at ~17.5 ka and ~15 ka, getting younger westward.
- Landform record occurring in the investigated part of Poland (subglacial meltwater corridors, subglacial and ice-marginal valleys, eskers) suggests that dynamic behavior of the retreating ice sheet with frequent oscillations of the ice margin may have been induced by the influence of substantial amounts of subglacial meltwater, which could also have triggered asynchronous dynamics of individual ice streams/ice lobes.
- The complex development of ice-marginal formations during glacial cycles largely hinders the correlation of individual ice-marginal belts and the dating of these features as distinct phases of glaciation or deglaciation. As a result, regional correlations of synchronous ice sheet limits along the southern margin of the last FIS are extremely difficult, if not entirely unfeasible.

Funding

This work was supported by the National Science Center in Poland [grant no. 2014/15/D/ST10/04113 to Karol Tylmann] and funding from Department of Geomorphology and Quaternary Geology, University of Gdańsk. The ASTER AMS national facility (CEREGE, Aix-en-Provence) is supported by the INSU/CNRS, the ANR through the “Projets thématiques d'excellence” program for the “Equipements d'excellence” ASTER-CEREGE action and IRD.

Author contribution

The contribution of co-authors to the manuscript is the following: K. Tylmann – conceptualization, collecting data, samples preparation, data analysis, interpreting and discussing results, writing (first draft, editing and proof-reading), V. Rinterknecht – collecting data, samples preparation, data analysis, writing (editing and proof-reading), P.P. Woźniak - collecting data, writing (editing and proof-reading), D. Moskalewicz - collecting data, A. Bielicka-Giełdoń – sample analysis (ICP OES), ASTER Team (G. Aumaître, K. Keddadouche, F. Zaïdi) – samples analysis (AMS measurements of ^{10}Be/^{9}Be ratios).

Declaration of competing interest

The authors declare that they have no known competing financial interests or personal relationships that could have influenced the work reported in this paper.

Acknowledgements

We are very grateful to the Regional Directorates of Environmental Protection and local communes offices for permissions for sampling large erratics protected by law.

References

1. Arnold, M., Merchel, S., Bourlés, D.L., Braucher, R., Benedetti, L., Finkel, R.C., Aumaître, G., Gottdang, A., Klein, M., 2010. The French accelerator mass spectrometry facility ASTER: Improved performance and developments. Nuclear Instruments and Methods in Physics Research B 268, 1954–1959.
2. Balco, G., Stone, J.O., Lifton, N.A., Dunai, T.J., 2008. A complete and easily accessible means of calculating surface exposure ages or erosion rates from ^{10}Be and ^{26}Al measurements. Quaternary Geochronology 3, 174–195.
3. Błaszkiewicz, M., 2011. Timing of the final disappearance of permafrost in the central European Lowland, as reconstructed from the evolution of lakes in N Poland. Geological Quarterly 55, 361–374.
4. Błaszkiewicz, M., Tylmann, K., 2023. Tunnel valleys of the Tuchola Forest and Kashubian Lake District. In: Migoń, P., Jancewicz, K. (eds) Landscapes and landforms of Poland. Springer, 615–632.
5. Borchers, B., Marrero, S., Balco, G., Caffee, M., Goehring, B., Lifton, N., Nishiizumi, K., Philips, F., Schaefer, J., Stone, J., 2016. Geological calibration of spallation production rates in the CRONUS-Earth project. Quaternary Geochronology 31, 188–198.
6. Boulton, G.S., Dongelmans, P., Punkari, M., Broadgate, M., 2001. Palaeoglaciology of an ice sheet through a glacial cycle: the European ice sheet through the Weichselian. Quaternary Science Reviews 20, 591–625.
7. Börner, A., Gehrmann, A., Hüneke, H., Kenzler, M., Lorenz, S., 2019. The Quaternary sequence of Mecklenburg-Western Pomerania: areas of specific interest and ongoing investigations. DEUQUA Special Publications 2, 1–10.
8. Bradwell, T., Small, D., Fabel, D., Smedley, R.K., Clark, C.D., Saher, M.H., Callard, S.L., Chiverrell, R.C., Dove, D., Moreton, S.G., Roberts, D.H., Duller, G.A.T., Ó Cofaigh, C. 2019. Ice-stream demise dynamically conditioned by trough shape and bed strength. Science Advances 5, 10.1126/sciadv.aau1380.
9. Braucher, R., Guillou, V., Bourlès, D. L., Arnold, M., Aumaître, G., Keddadouche, K., Nottoli, E., 2015. Preparation of ASTER in-house ^{10}Be/^{9}Be standard solutions. Nuclear Instruments and Methods in Physics Research B 361, 335–340.
10. Bülow, K.V., 1924. Die Diluviallandschaft im nordostlichen Hinterpommern. Jahrbuch d. Preuss. Geologischen Landesanstalt 45, 317–344.
11. Chmeleff, J., von Blanckenburg, F., Kossert, K., Jakob, D., 2010. Determination of the ^{10}Be half-life by multicollector ICP-MS and liquid scintillation counting. Nuclear Instruments and Methods in Physics Research Section B: Beam Interactions with Materials and Atoms 268, 192–199.
12. Cuzzone, J.K., Clark, P.U., Carlson, A.E., Ullman, D.J., Rinterknecht, V.R., Milne, G.A., Lunkka, J.-P., Wohlfarth, B., Marcott, S.A., Caffee, M., 2016. Final deglaciation of the Scandinavian Ice Sheet and implications for the Holocene global sea-level budget. Earth Planetary Science Letters 448, 34–41.
13. Denton, G.H., Anderson, R.F., Toggweiler, J.R., Edwards, R.L., Schaefer, J.M., Putnam, A.E., 2010. The Last Glacial Termination. Science 328, 1652–1656.

14. Ehlers, J., Grube, A., Stephan, H.-J., Wansa, S., 2011. Pleistocene glaciations of north Germany–new results. In: J. Ehlers, P.L. Gibbard, P.D. Hughes (Eds.), Quaternary Glaciations - Extent and Chronology: A Closer Look, Elsevier Amsterdam, 149–162.
15. Giedrojć-Juraha, S., 1949. Moreny czołowe okolic jeziora Gardno. Czasopismo Geograficzne 20, 239–244.
16. Greenwood, S. L., Avery, R. S., Gyllencreutz, R., Regnéll, C., Tylmann, K., 2024. Footprint of the Baltic Ice Stream: geomorphic evidence for shifting ice stream pathways. Boreas 53, 4–26.
17. Greenwood, S.L., Clark, C.D., 2009. Reconstructing the last Irish Ice Sheet 1: changing flow geometries and ice flow dynamics deciphered from the glacial landform record. Quaternary Science Reviews 28, 3085–3100.
18. Greenwood, S.L., Clark, C.D., Wilson, A.S.G., 2007. Formalising an inversion methodology for reconstructing ice-sheet retreat patterns from meltwater channels: Application to the British Ice Sheet. Journal of Quaternary Science 22, 637–645.
19. Hermanowski, P., Piotrowski, J.A., 2022. Origin of glacial curvilineations by subglacial meltwater erosion: Evidence from the Stargard drumlin field, Poland. Earth Surface Processes and Landfroms 48, 282–294.
20. Heyman, J., Applegate, P.J., Blomdin, R., Gribenski, N., Harbor, J.M., Stroeven, A.P., 2016. Boulder height - exposure age relationships from a global glacial ^{10}Be compilation. Quaternary Geochronology 34, 1–11.
21. Hoffman, M., Price, S., 2014. Feedbacks between coupled subglacial hydrology and glacier dynamics. Journal of Geophysical Research: Earth Surface 119, 414–436.
22. Hughes, A.L.C., Clark, C.D., Jordan, C.J., 2014. Flow-pattern evolution of the last British Ice Sheet. Quaternary Science Reviews 89, 148–168.
23. Hughes, A.L.C., Gyllencreutz, R., Lohne, Ø.S., Mangerud, J., Inge, J., 2016. The last Eurasian ice sheets – a chronological database and time-slice reconstruction, DATED-1. Boreas 45, 1–45.
24. Hughes, A.L.C., Winsborrow, M.C.M., Greenwood, S.L., 2021. European ice sheet complex evolution during the last glacial maximum (29-19 ka). In: Palacios, D., Hughes, P.D., García-Ruiz, J.M., Andres, N. (Eds.), European Glacial Landscapes. Maximum Extent of Glaciations. Elsevier, pp. 361–372.
25. Jasiewicz, J., 1999. Glacitektoniczna struktura dupleksu (gardzieńska morena czołowa, klif w Dębinie na zachód od Rowów). In: R.K. Borówka, Z. Młynarczyk, A. Wojciechowski (eds.) Ewolucja geosystemów nadmorskich południowego Bałtyku. Bogucki Wydawnictwo Naukowe, Poznań-Szczecin, 87–93.
26. Kalińska, E., Weckwerth, P., Alexanderson, H., Piotrowski, J.A., Wysota, W., 2025. OSL dating of glacial outburst flood deposits in NE Poland and their bleaching problem inferred from the landform-sediment associations and regional context. Quaternary Research 124, 26–46.
27. Kalm, V., 2012. Ice-flow pattern and extent of the last Scandinavian Ice Sheet southeast of the Baltic Sea. Quaternary Science Reviews 44, 51–59.
28. Kamleitner, S., Ivy-Ochs, S., Salcher, B., Reitner, J.M., 2024. Reconstructing basal ice flow patterns of the Last Glacial Maximum Rhine glacier (northern Alpine foreland)

based on streamlined subglacial landforms. Earth Surface Processes and Landforms 49, 746–769.

29. Kehew, A.E., Piotrowski, J.A., Jørgensen, F., 2012. Tunnel valleys: Concepts and controversies – A review. Earth-Science Reviews 113, 33–58.
30. Kelley, S.E., Briner, J.P., O'Hara, S.L., 2018. Assessing ice margin fluctuations on differing timescales: Chronological constraints from Sermeq Kujatdleq and Nordenskiöld Gletscher, central West Greenland. The Holocene 28, 1160–1172.
31. Kjær, K.H., Larsen, E., van der Meer, J., Ingólfsson, Ó., Krüger, J., Benediktsson, Í.Ö., Knudsen, C.G., Schomacker, A., 2006. Subglacial decoupling at the sediment/bedrock interface: A new mechanism for rapid flowing ice. Quaternary Science Reviews 25, 2704–2712.
32. Kłysz, P., 2003. Maximum limits of the Baltic ice-sheet during the Pomeranian phase in the Drawskie Lakeland. Quaestiones Geographicae 22, 29–42.
33. Korschinek, G., Bergmaier, A., Faestermann, T., Gerstmann, U.C., Knie, K., Rugel, G., Wallner, A., Dillmann, I., Dollinger, G., von Gostomski, C.L., 2010. A new value for the half-life of ^{10}Be by Heavy-Ion Elastic Recoil Detection and liquid scintillation counting. Nuclear Instruments and Methods in Physics Research Section B: Beam Interactions with Materials and Atoms 268, 187–191.
34. Kozarski, S., 1986. Skale czasu a rytm zdarzeń geomorfologicznych vistulianu na Niżu Polskim. Czasopismo Geograficzne 57, 247–270.
35. Kozarski, S., 1995. Deglacjacja Polski północno-zachodniej: warunki środowiska i transformacja geosystemu (20 ka–10 ka BP). Dokumentacja Geograficzna 1, 1–82.
36. Krauß, N., Börner, A., Kenzler, M., 2025. Geochronological investigations at the maximum extent of the Fennoscandian Ice Sheet during the Late Weichselian glaciation in northern Germany. Boreas, https://doi.org/10.1111/bor.12695.
37. Lal, D., 1991. Cosmic ray labeling of erosion surfaces: In situ nuclide production rates and erosion models. Earth Planetary Science Letters 104, 424–439.
38. Larsen, E., Fredin, O., Lysså, A., Amantov, A., Fjeldskaar, W., Ottesen, D., 2016. Causes of time-transgressive glacial maxima positions of the last Scandinavian Ice Sheet. Norwegian Journal of Geology 96, 159–170.
39. Lesemann, J.E., Piotrowski, J.A., Wysota, W., 2010. 'Glacial curvilineations': New glacial landforms produced by longitudinal vortices in subglacial meltwater flows. Geomorphology 120, 153–161.
40. Lesemann, J.E., Piotrowski, J.A., Wysota, W., 2014. Genesis of the 'glacial curvilineations' landscape by meltwater processes under the former Scandinavian Ice Sheet, Poland. Sedimentary Geology 312, 1–18.
41. Lewington, E.L.M., Livingstone, S.J., Sole, A.J., Clark, C.D., Ng, F.S.L., 2020. A model for interaction between conduits and surrounding hydraulically connected distributed drainage systems within the ablation zone of the Keewatin Ice Divide, Canada. The Cryosphere 14, 2949–2968.
42. Lüthgens, C., Hardt, J., Böse, M., 2020. Proposing a new conceptual model for the reconstruction of ice dynamics in the SW sector of the Scandinavian Ice Sheet (SIS) based on the reinterpretation of published data and new evidence from optically

stimulated luminescence (OSL) dating. E&G Quaternary Science Journal 69, 201–223.

43. Małka, A., Jurys, L., Maszloch, E., Wirkus, K., Pączek, U., 2003. Szczegółowa mapa geologiczna Polski w skali 1: 50 000, arkusz Żarnowiec – aktualizacja. PIG–PIB, Warszawa.
44. Marks, L., 2002. Last glacial maximum in Poland. Quaternary Science Reviews 21, 103–110.
45. Marks, L., 2012. Timing of the Late Vistulian (Weichselian) glacial phases in Poland. Quaternary Science Reviews 44, 81–88.
46. Marks, L., 2015. Last deglaciation of northern Continental Europe. Cuadernos Investigacion Geografica 41, 279–297.
47. Marks, L., Ber, A., Gogołek, W., Piotrowska, K., 2006 (eds.). Mapa Geologiczna Polski 1:500 000. Ministerstwo Środowiska, PIG-PIB, Warszawa.
48. Marks, L., Dzierżek, J., Janiszewski, R., Kaczorowski, J., Lindner, L., Majecka, A., Makos, M., Szymanek, M., Tołoczko-Pasek, A., Woronko, B., 2016. Quaternary stratigraphy and palaeogeography of Poland. Acta Geologica Polonica 66, 403–427.
49. Merchel, S., Arnold M., Aumaître, G., Benedetti, L., Bourlès, D.L., Braucher, R., Alfimov, V., Freeman, S.P.H.T., Steier, P., Wallner, A., 2008. Towards more precise ^{10}Be and ^{36}Cl data from measurements at the 10^{-14} level: Influence of sample preparation. Nuclear Instruments and Methods in Physics Research Section B: Beam Interactions with Materials and Atoms 266, 4921–4926.
50. Merchel, S., Herpers, U., 1999. An update on radiochemical separation techniques for the determination of long-lived radionuclides via accelerator mass spectrometry, Radiochimica Acta 84, 215–220.
51. Mojski, J.E., 2000. The evolution of the southern Baltic coastal zone. Oceanologia 42, 285–303.
52. Mojski, J.E., 2005. Ziemie polskie w czwartorzędzie. Zarys morfogenezy. Państwowy Instytut Geologiczny, Warszawa.
53. Mörner, N.A., Floden T., Beskow B., Elhammer A., Haxner H., 1977. Late Weichselian deglaciation of the Baltic. Baltica 6, 33–51.
54. Niewiarowski, W., Olszewski, A., Wysota, W., 1995. The role of subglacial features in glacial morphogenesis of the Kujawy-Dobrzyń subphase area in the southern and eastern part of the Chełmno–Dobrzyń Lakeland. Quaternary Studies in Poland 13, 65–76.
55. Patton, H., Hubbard, A., Bradwell, T., Glasser, N.F., Hambrey, M.J., Clark, C.D., 2013. Rapid marine deglaciation: asynchronous retreat dynamics between the Irish Sea Ice Stream and terrestrial outlet glaciers. Earth Surface Dynamics 1, 53–65.
56. Pazdur, M., Walanus, A., 1979, The Konin-Maliniec site: Age assesment by radio-carbon method. Symposium on Vistulian Stratigraphy, Poland. Guide-book of excursion, Warszawa.
57. Petelski, K., 1985. Budowa geologiczna moreny czołowej i niecki końcowej lobu gardzieńskiego. Biuletyn Instytutu Geologicznego 348, 89–121.

58. Punkari, M., 1997. Glacial and glaciofluvial deposits in the interlobate areas of the Scandinavian ice sheet. Quaternary Science Reviews 16, 741–753.

59. Roman, M., 2019. Ice-flow directions of the last Scandinavian Ice Sheet in central Poland. Quaternary International 501, 4–20.

60. Rotnicki K., Borówka R. K., 1994. Stratigraphy, palaeogeography and dating of the North Polish Stage in the Gardno-Łeba Coastal Plain. In: K. Rotnicki (ed.) Changes of the Polish Coastal Zone, A. Mickiewicz University, Poznań, 84–88.

61. Rotnicki, K., Borówka, K., 1995. The last cold period in the Gardno-Łeba Coastal Plain. Journal of Coastal Research. Special Issue No. 22, 225–229.

62. Rychel, J., Sokołowski, R.J., Sieradz, D., Hrynowiecka, A., Mirosław-Grabowska, J., Sienkiewicz, E., Niska, M., Szymanek, M., Zbucki, Ł., Ciołko, U., Rogóż-Matyszczak, A., 2022. Late Pleniglacial – Late Glacial climate oscillations detected in the organic lacustrine succession at the Lipowo site, north-eastern Poland. Journal of Quaternary Science 38, 186–207.

63. Słowiński, M., Błaszkiewicz, M., Brauer, A., Noryśkiewicz, B., Ott, F., Tyszkowski, S., 2015. The role of melting dead ice on landscape transformation in the early Holocene in Tuchola Pinewoods, North Poland. Quaternary International 388, 64–75.

64. Smedley, R.K., Chiverrell, R.C., Ballantyne, C.K., Burke, M.J., Clark, C.D., Duller, G.A.T., Fabel, D., McCarroll, D., Scourse, J.D., Small, D., Thomas, G.S.P., 2017. Internal dynamics condition centennial-scale oscillations in marine-based ice-stream retreat. Geology 45, 787–790.

65. Spagnolo, M., Clark, C.D., Ely, J.C., Greenwood, S.L., Hughes, A.L.C., Moreton, S.G., Stokes, C.R., 2014. Size, shape, and spatial arrangement of mega-scale glacial lineations. Sedimentary Geology 338, 56–70.

66. Stankowska, A., Stankowski, W., 1979, The Vistulian till covering stagnant water sediments with organic sediments. Symposium on Vistulian Stratigraphy, Poland, Guide-book of excursion, Warszawa.

67. Stone, J., 2000. Air pressure and cosmogenic isotope production. Journal of Geophysical Research 105, 23753–23760.

68. Storrar, R.D., Stokes, C.R., Evans, D.J.A., 2014. Increased channelization of subglacial drainage during deglaciation of the Laurentide Ice Sheet. Geology 42, 239–242.

69. Stroeven, A.P., Hättestrand, C., Kleman, J., Heyman, J., Fabel, D., Fredin, O., Goodfellow, B.W., Harbor, J.M., Jansen, J.D., Olsen, L., Caffee, M.W., Fink, D., Lundqvist, J., Rosqvist, G.C., Strömberg, B., Jansson, K.N., 2016. Deglaciation of Fennoscandia. Quaternary Science Reviews, 147, 91–121.

70. Sylwestrzak, J., 1978. Rozwój sieci dolinnej na Pomorzu pod koniec plejstocenu. Gdańskie Towarzystwo Naukowe, Ossolineum.

71. Szuman, I., Kalita, J.Z., Ewertowski, M.W., Clark, C.D., Livingstone, S.J., 2021. Dynamics of the last Scandinavian Ice Sheet's southernmost sector revealed by the pattern of ice streams. Boreas 50, 764–780.

72. Thøgersen, K., Gilbert, A., Bouchayer, C., Schuler, T.V., 2024. Glacier Surges Controlled by the Close Interplay Between Subglacial Friction and Drainage. Journal of Geophysical Research: Earth Surface129, e2023JF007441.

73. Tomkins, M. D., Dortch, J. M., Hughes, P., Huck, J. J., Pallàs, R., Rodés, Á., Allard, J. L., Stimson, A. G., Bourlès, D., Rinterknecht, V., Jomelli, V., Rodríguez-Rodríguez, L., Copons, R., Barr, I. D., Darvill, C. M., Bishop, T., 2021. Moraine crest or slope: An analysis of the effects of boulder position on cosmogenic exposure age. Earth and Planetary Science Letters, 570, 117092.

74. Tylmann, K., Uścinowicz, Sz., 2022. Timing of the last deglaciation phases in the southern Baltic area inferred from Bayesian age modeling. Quaternary Science Reviews, 287, 107563.

75. Tylmann, K., Rinterknecht, V.R., Woźniak, P.P., Bourlès, D., Schimmelpfennig, I., Guillou, V., ASTER Team, 2019. The Local Last Glacial Maximum of the southern Scandinavian Ice Sheet front: Cosmogenic nuclide dating of erratics in northern Poland. Quaternary Science Reviews 219, 36–46.

76. Tylmann, K., Rinterknecht, V., Woźniak, P.P., Guillou V., ASTER Team, 2022. Asynchronous dynamics of the last Scandinavian Ice Sheet along the Pomeranian ice-marginal belt: A new scenario inferred from surface exposure ^{10}Be dating. Quaternary Science Reviews 294, 107755.

77. Tylmann, K., Wysota, W., Rinterknecht, V., Moska, P., Bielicka-Giełdoń, A., ASTER Team, 2024. Millennial-scale fluctuations of palaeo-ice margin at the southern fringe of the last Fennoscandian Ice Sheet. The Cryosphere 18, 1889–1909.

78. Uścinowicz, Sz., 1999. Southern Baltic area during the last deglaciation. Geological Quarterly 43, 137–148.

79. Uścinowicz, Sz., 2014. Baltic Sea Continental Shelf. In: F. Chiocci, A. Chivas (eds.) Continental Shelves of the World, Their Evolution During Last Glacio-Eustatic Cycle. Geological Society Memoir No. 41, London, 69–89.

80. Uścinowicz, Sz., Adamiec, G., Bluszcz, A., Jegliński, W., Jurys, L., Miotk-Szpiganowicz, G., Moska, P., Pączek, U., Piotrowska, P., Poręba, G., Przezdziecki, P., Uścinowicz, G., 2019. Chronology of the last ice sheet decay on the southern Baltic area based on dating of glaciofluvial and ice-dammed lake deposits. Geological Quarterly 63, 192–207.

81. Weckwerth, P., Wysota, W., Piotrowski, J.A., Adamczyk, A., Krawiec, A., Dąbrowski, M., 2019. Late Weichselian glacier outburst floods in North-Eastern Poland: landform evidence and palaeohydraulic significance. Earth Science Reviews 194, 216–233.

82. Winsborrow, M.C.M. Hughes, A.L.C., Greenwood, S.L., 2023. European Ice Sheet Complex evolution during main deglaciation (18.9–14.6 ka). In: D. Palacios, P.D. Hughes, J.M. García-Ruiz, N. Andrés (eds.) European Glacial Landscapes. The Last Deglaciation. Elsevier, 71–83.

83. Woldstedt, P., 1925. Die grosser Endmoränenzüge Norddeutschland. Zeitschrift der Deutschen Geologischen Gesellschaft 77, 172–184.

84. Woldstedt, P., 1935. Über die Geschichte des Küstriner Beckens und der Eberswalder Pforte. Jahrbuch der Königlichen Preussischen Geologischen Landesanstalt 56, 274–291.

85. Woźniak, P.P., Czubla, P., 2015. The Late Weichselian glacial record in northern Poland: A new look at debris transport routes by the Fennoscandian Ice Sheet. Quaternary International 386, 3–17.

86. Wysota, W., Molewski, P., Sokołowski, R.J., 2009. Record of Vistula ice lobe advance in the Late Weichselian glacial sequence in north-central Poland. Quaternary International 207, 26–41.

Supplementary materials

Dynamics of the last ice sheet on the northern fringe of Poland: reconstruction inferred from landform analysis and ^{10}Be surface exposure dating

Karol Tylmann, Vincent Rinterknecht, Piotr P. Woźniak, Damian Moskalewicz, Aleksandra Bielicka-Giełdoń, ASTER Team

Figure: Fig. S1-S2

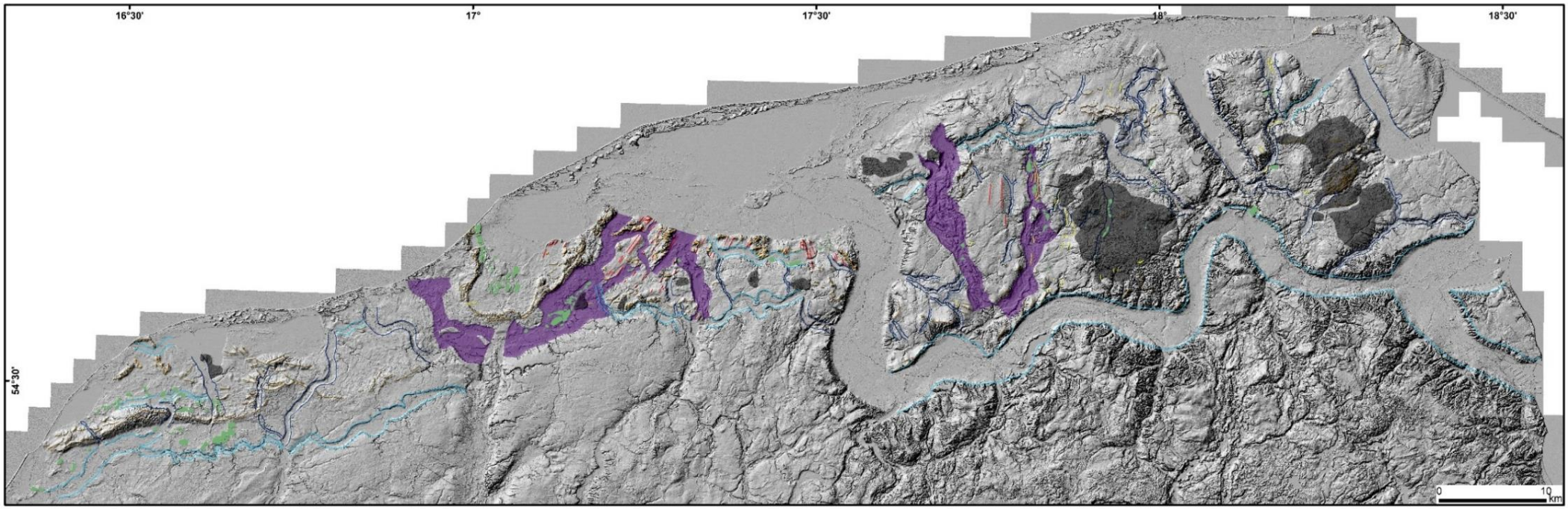

Fig. S1 Glacial landforms mapped in the study area – high-resolution map. Explanations for symbols and colors available as a legend in Fig. 3B in the article.

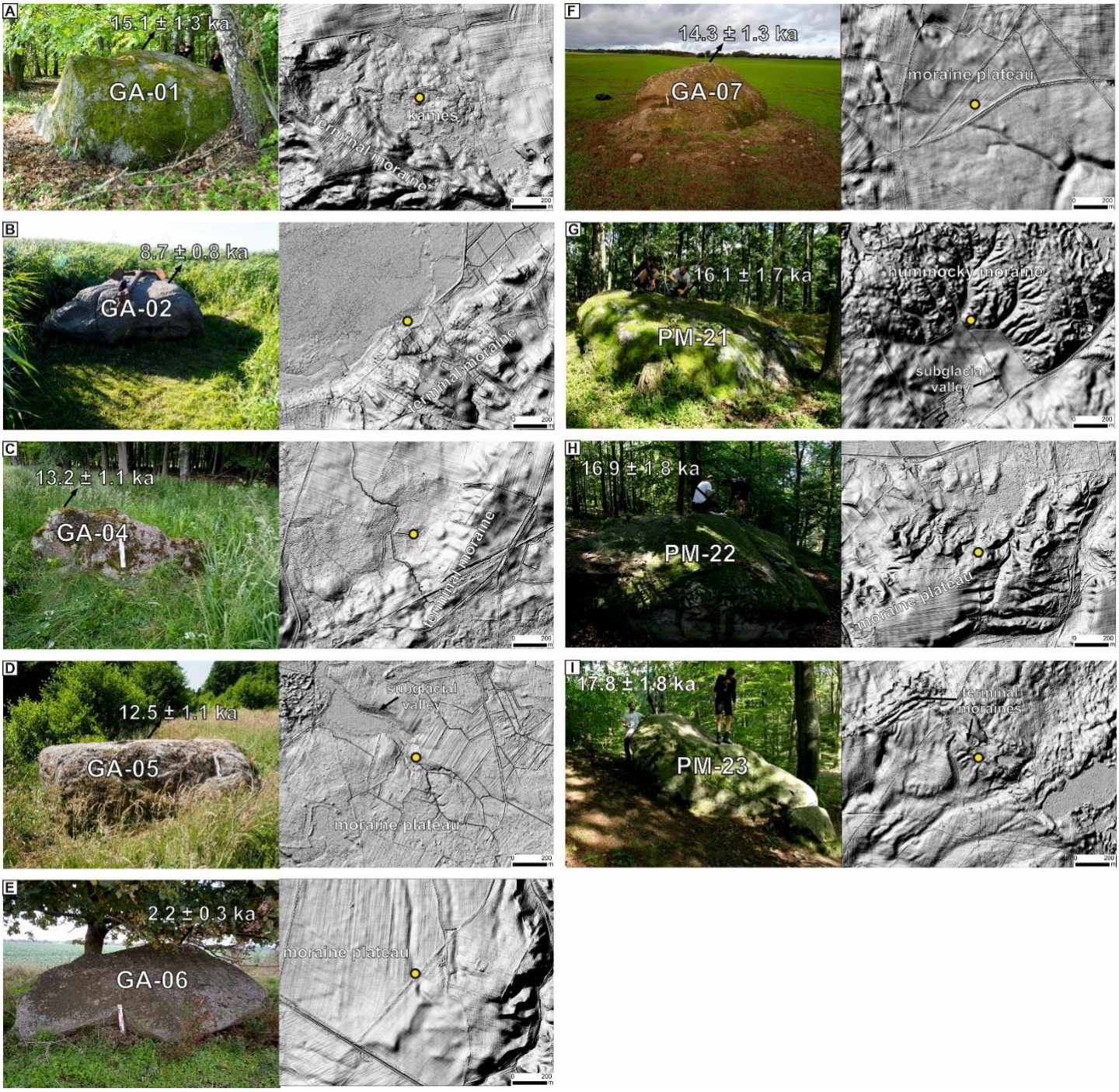

Fig. S2 Pictures and detailed locations on LiDAR DEM of erratic boulders sampled for ^{10}Be dating.